Project of Strategic Interest NEXTDATA

WP1.2
(Coordinator: Marco Doveri, IGG-CNR)

D1.2A - Report on geological, hydrogeological and geochemical features and data of selected Apennines and Alpine aquifer systems

Authors: Marco Doveri, Brunella Raco, Matia Menichini, Barbara Nisi, Andrea Irace, Giulio Masetti, Matteo Lelli

IGG-CNR

This deliverable focus on geological, hydrogeological and geochemical data and information concerning aquifer systems located in central and northern Apennines and western Alps. It also provides a discussion on trends of some quantity and quality parameters of groundwater.

Table of contents

1. INTRODUCTION

The Task 1 of WP1.2 focus on groundwater, which represents, globally, the main resource in term of water supply. Worldwide, more than 2 billion people depend on groundwater for their daily water use (Hiscock, 2011). In many areas groundwater bodies represent the most important and safest source for drinking water (Zhu and Balke, 2008; Baoxiang and Fanhai, 2011). In the European countries, for example, the groundwater exploitation provides water for human consumption for 70% of the population on average (Martínez et al., 2008). Groundwater withdrawals supply 40% of industrial water (WBCSD, 2006) and groundwater use for irrigation is also significant and increasing. Siebert et al., 2010 estimated that, globally, the 38% of the area equipped for irrigation is irrigated by groundwater. Also in Italy groundwater represents the main source for satisfying water demand, even reaching 80% of water supplied for human consumption. Moreover, the exploitation of groundwater bodies will likely increase both for the key role played by aquifers for mitigating the climate change/variability and for the significant increasing of the global water demand, which has been predicted because of the future economic expansion, population growth, and urbanization (Rosegrant et al., 2002).

Despite this, and unlike surface waters, groundwater bodies have not been widely studied, and there is a general paucity of information, especially in relation to climate change. Although groundwater systems are more resilient to climate change than surface waters, they are however affected both directly and indirectly (Tylor et al., 2013), especially referring to local groundwater flow with low travel time (Fan, 2015). Doveri et al. (2017; 2018a) highlight as in Italy some groundwater systems are indicating a decline of groundwater yields over the last two decades, as a consequence of the recharge decreasing that in some systems even causes a significant releasing of water from storage reserves.

An increasing of knowledge on groundwater, including the estimation of the entity of the above-mentioned effects, is mandatory for a reliable management of this crucial resource, which must be protected by suitable actions in order to guarantee safe water supplying for next generations (Doveri et al., 2016).

In order to address the lacks of knowledge on groundwater systems, the Task 1 of the WP 1.2 deal with groundwater quantity and quality issues, referring to three selected aquifer systems that develop (Fig 1.1) in Apennines (Mt. Amiata and Apuan Alps systems) and Alpine zones (foothill system of the Piedemont). Data and information derive from studies and researches chiefly performed in close cooperation with water management companies and authorities, as well as from monitoring activities institutionally performed by regional governments and environmental agencies. The conceptual model of aquifers is accounted by comparing physical and chemical features. Furthermore, numerical models are developed throughout either empirical or physically-based approach, accordingly the hydrodynamic conditions of aquifers and the availability of data and information. The attempt is also to make the approach adopted during this work a reference strategy for investigating mountain aquifers.

This deliverable regards the first part of the Task 1, and particularly it describes the main geological, hydrogeological and geochemical features of the aquifers, providing also a synthesis of data into the conceptual models of these systems.

An analysis of the continuous monitoring data is also presented for quantitative and or qualitative groundwater parameters, according to the availability of data in different cases.

This document mainly focus on the Monte Amiata and Apuan Alps aquifer systems, postponing the discussion of the alpine system until next deliverable.

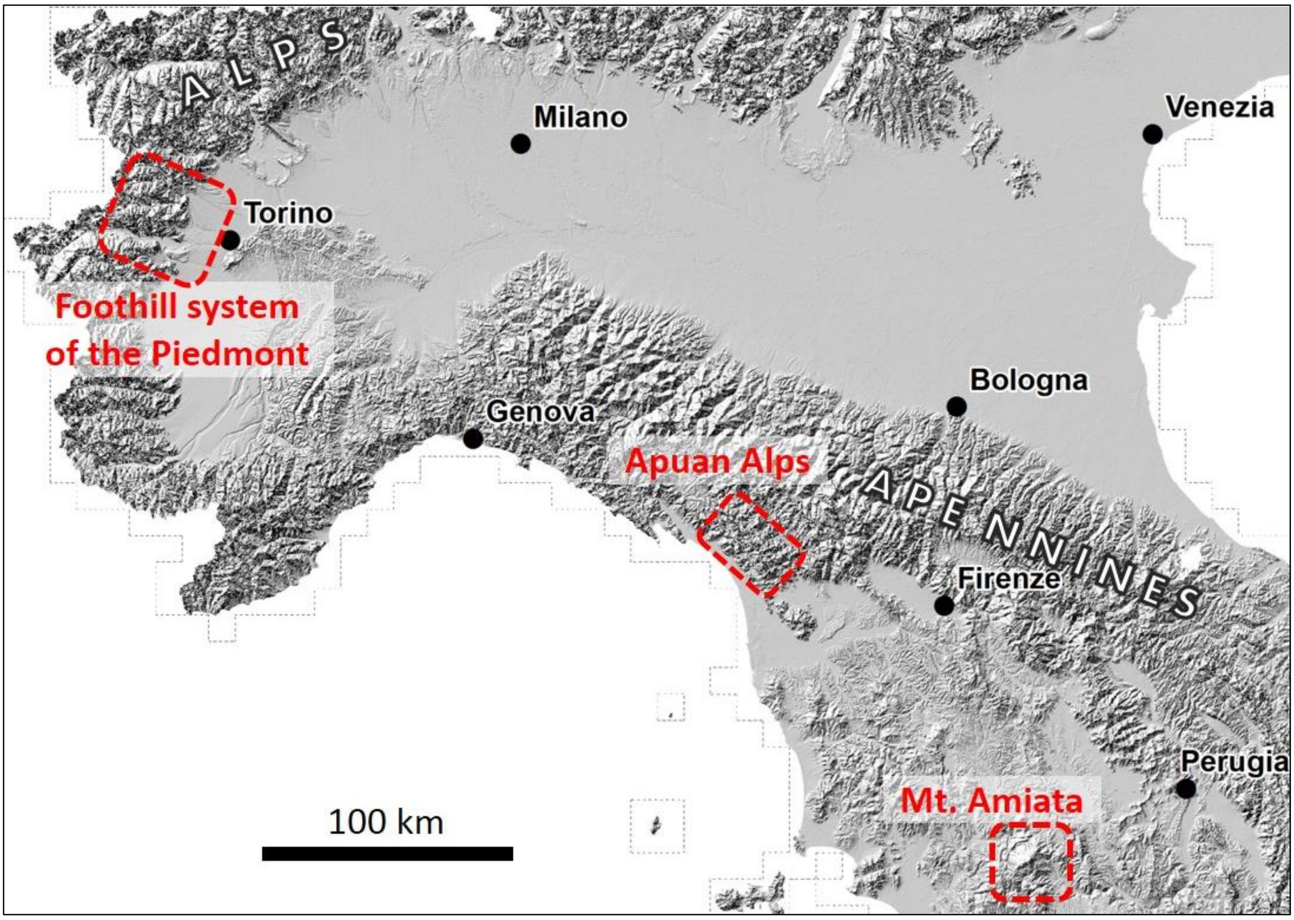

Fig. 1.1 – Apennine and Alps zones in which aquifer systems exanimated in the project extend.

2. THE MT. AMIATA AQUIFER SYSTEM

2.1. Geological, hydrogeological and geochemical setting

Mt. Amiata (1738 m a.s.l.) is a Quaternary volcano located in Southern Tuscany (central Italy) and covers an area of about 80 km^2 (Fig. 2.1). It belongs to the inner part of the Central Apennine, a NE-verging thrust and fold belt developed during the Tertiary, in a continental collisional setting (Boccaletti et al., 1971; 1981; Molli, 2008 and references therein), and successively (from the Middle Miocene) affected by extensional processes (Jolivet et al., 1994; Carmignani et al., 1995; Brunet et al., 2000). The geology of Mt. Amiata area is characterized by a structural stacking strongly reworked by extensional tectonics, to which the emplacement of Neogene-Quaternary “granitic” magmatic body at depths of about 6-7 km is related (Batini et al., 1986; Acocella, 2000). This process is responsible of the volcanic activity of the period ranging from 300 to 190 ka (Ferrari et al., 1996), as well as of the high heat flow (Baldi et al., 1995) that makes the area interesting from a geothermal point of view. Two geothermal fields are exploited at Bagnore and Pian Castagnaio, at SW and SE of Mt. Amiata (Fig. 2.1).

The geological sequence is represented, from top to bottom, by volcanics, Neogene and Quaternary deposits, Ligurian and Tuscan complexes, and the metamorphic Paleozoic basement of the Tuscan Nappe (Brogi et al., 2008; Marroni et al., 2015). The volcanic rocks are tied to two periods of eruptive activity that result in two main groups of volcanics. The latter are respectively named Basal Trachydacitic Complex (BTC) and Domes and Lava flow Complex (DLC) by Ferrari et al. (1996), and later renamed Bagnore Synthem and Monte Amiata Synthem by Principe et al. (2017). The Neogene and Quaternary deposits consist of continental and marine sediments mainly represented by clay. The Ligurian complexes in this zone chiefly consist of shaly lithologies and, generally, they directly overlay the Triassic evaporates and carbonates of the lower part of Tuscan Nappe. Only locally the Tuscan Nappe is present with the completed sequence, including Jurassic carbonates, Middle Jurassic-Cretaceous pelagic carbonates and cherts, Cretaceous-Oligocene pelagic shales, marls and limestones and Upper Oligocene-Lower Miocene siliciclastic turbidites. The Paleozoic basement is mainly made up by phyllites and metasandstones.

As a result of the geological setting, in the Mt. Amiata area four main hydrogeological units are recognizable from top to bottom (Fig. 2.1; Doveri & Menichini, 2017):

- the Monte Amiata volcanics that tanks to their high permeability host a very important aquifer (Mt. Amiata acquifer), with huge water resources mainly drained by several contact springs;
- a shaly-dominant sequence characterized by an overall permeability of low degree, which makes possible only local groundwater flow (Doveri & Mussi, 2014). It plays the role of impervious substratum for the overlying Mt. Amiata aquifer, as well as the role of cap-rock respect to the underlying regional evaporitic-carbonate reservoir;
- a regional evaporitic-carbonate reservoir, which is diffusely interested by thermal groundwater flow, resulting from the combined effect of high rocks permeability, high geothermal gradient of the region, and confinement of the reservoir on most part of the

area. In the zone close to Mt. Amiata it hosts two geothermal fields (named shallow geothermal fields, at Bagnore and Piancastagnaio);

- a Paleozoic basement, which is mainly impermeable, excluding fractured zones that are exploited by deep geothermal wells (deeper geothermal fields, at Bagnore and Piancastagnaio).

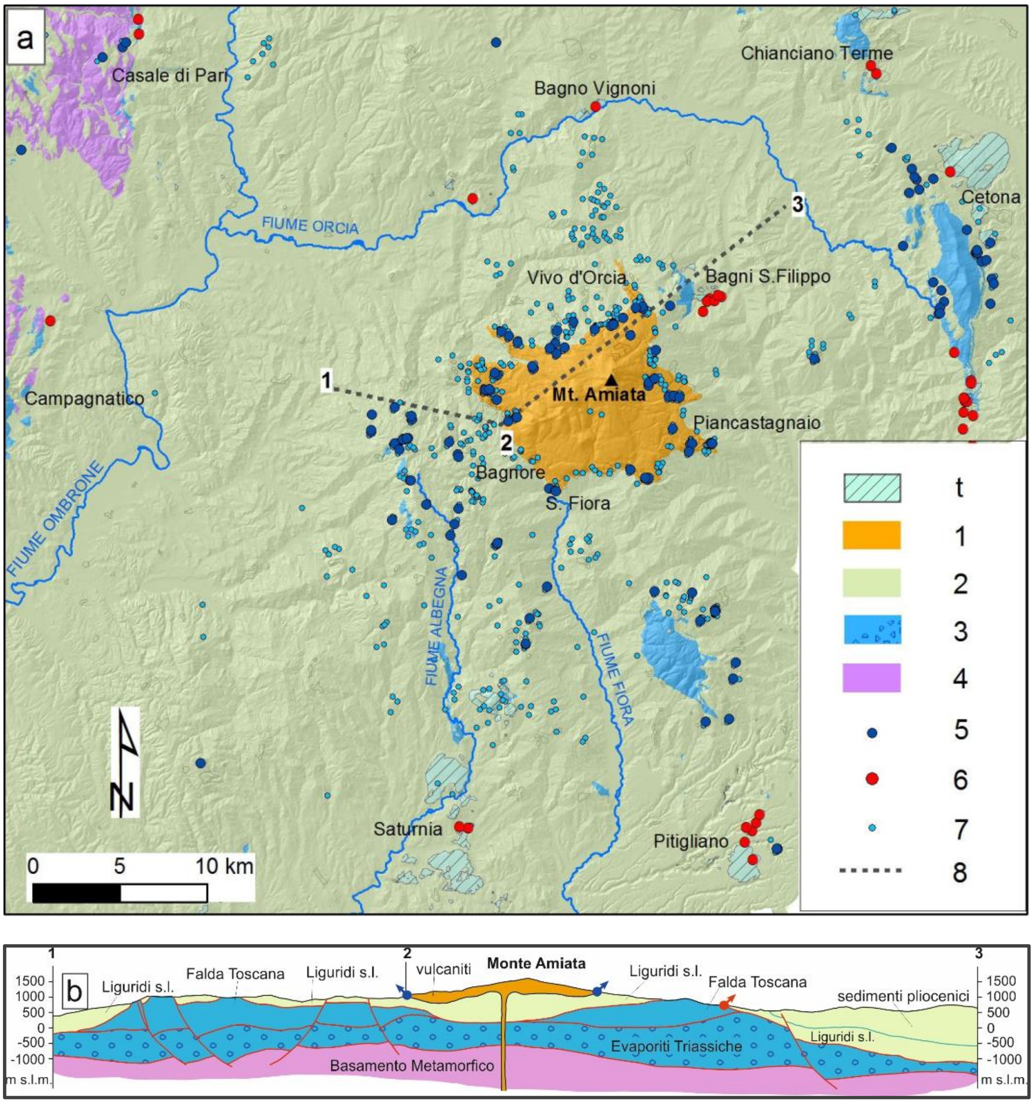

Fig. 2.1 - Hydrogeological sketch map (a) and section (b) of the Monte Amiata region (from Doveri & Menichini., 2017). Legend: t - travertine; 1 – Mt. Amiata aquifer; 2 - substratum of the Mt. Amiata aquifer and cap-rock of the carbonate-evaporitic reservoir; 3 - carbonate-evaporitic reservoir (in the section, the sandstones and shales of the upper part of the Tuscan Nappe are also involved); 4 - metamorphic basement; 5 - drinking water spring; 6 - thermal spring; 7 - other cold springs; 8 - trace of the cross section.

As a whole, the Mt. Amiata aquifer system is an unconfined aquifer. Nevertheless, in the inner part Doveri et al. (2012) e Doveri & Menichini (2017) distinguished a main basal aquifer, in semi-confined conditions, from local perched aquifers that originate small springs at altitudes relatively high (Fig. 2.2).

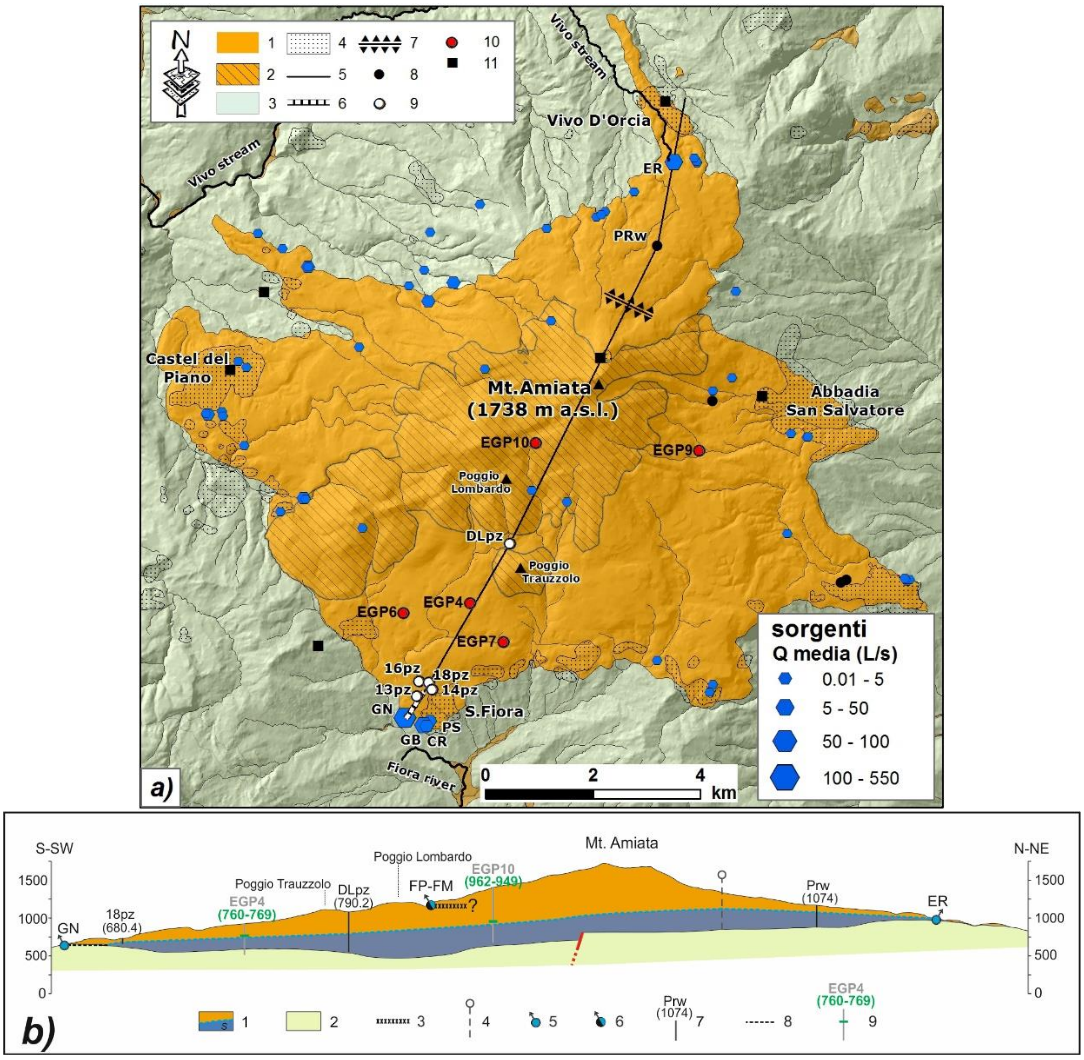

Fig. 2.2 - Hydrogeological sketch map (a) and section (b) of the Monte Amiata (from Doveri & Menichini, 2017). *Legend of the sketch map*; 1) and 2) volcanic rocks with medium-high permeability, respectively belonging to the Base Complex and Dome Complex, as defined by Ferrari et al. (1996); 3) shaly substratum with low to very low permeability; 4) main villages; 5) trace of the section; 6) artificial draining tunnel; 7) zone of the groundwater divide that separates GN groundwater system from the ER one; 8) drinking water pumping well; 9) piezometer; 10) piezometer recently constructed by Enel Green Power; 11) meteorological station. *Legend of the section*: 1) volcanics aquifer (*s* indicates the saturated zone, as indicated in Doveri et al., 2012); 2) substratum with low to very low permeability; 3) aquitard responsible of local perched aquifers; 4) groundwater divide; 5) contact spring; 6) perched spring; 7) well or piezometer (parenthesis include the a.s.l. groundwater level value measured on July 2011); 8) artificial draining tunnel; 9) piezometer recently constructed by Enel Green Power (green segments and numbers indicate the ranges of position and piezometric value registered at piezometer). Should be noted that the piezometric profile previously elaborated by Doveri et al. (2012) is consistent with the piezometric levels of the new piezometers.

According to Authors, this hydrogeological setting is tied to the presence of a lower-permeability limit between volcanics of the Bagnore Synthem and those of the Monte Amiata Synthem, likely corresponding to the surface of erosion and saprolithic weathering recognized by Principe et al. (2017). However, groundwater is mainly drained by several springs (more than 150 according to Barazzuoli et al., 1994) that are distributed all around the volcanic body, generally close to the contact between the volcanic rocks and the substratum (Fig. 2.2).

Two major groups of springs are located in the southern (close to the Santa Fiora village) and northern (close to the Vivo d'Orcia village) parts of the volcanic complex, respectively. Galleria Nuova (GN), Galleria Bassa (GB), Carolina (CR) and Peschiera (PS) springs represent the first group, which has a flow rate higher than 700 L/s in average (Dini et al., 2010; Doveri et al., 2012). The second group is essentially represented by the spring named Ermicciolo (ER), which has an average flow rate of about 100 L/s. Most springs is taped for supplying drinking water over a wide and densely populated area that encompasses the Siena and Grosseto districts and part of the Arezzo and Viterbo districts. In relation to a hydrologic period of more than fifty years, from an average rainfall on the aquifer of about 1220 mm/yr resulted a recharge very similar to the total output at springs and of the order of 50-55E06 m^3/y (Celico, 1987; Barazzuoli et al., 1994; Barazzuoli et al., 2014). Hence, the Authors concluded the Monte Amiata aquifer has not significant water loss throughout the substratum. The recent construction of six piezometers in the inner part of the volcanic body enabled to carry on tests and continuous monitoring of the water level, with consequent production of hydraulic and hydrodynamic data. By performing hydraulic tests Doveri et al. (2012; 2013a; 2013b) achieved value of K in the range 5.0E-06 ÷ 4.6E-05 m/s for the volcanites of the Bagnore Synthem. Moreover, by comparing hydrographs of springs and piezometers, and by performing piezometric measurements at selected points along a principal hydrogeological section (Galleria Nuova spring–Monte Amiata ridge-Ermicciolo spring), Doveri et al. (2012) elaborated a piezometric profile steered by experimental data and elaborations of the hydrogeological type. Latest data from new piezometers seems to validate such as profile (Fig. 2.2b). By elaborating data from piezometers and springs (Fig. 2.3), Doveri & Menichini (2017) pointed out the existence of very different hydrodynamic conditions within the aquifer, and particularly between the volcanites of the Bagnore Synthem and those of the Amiata Synthem.

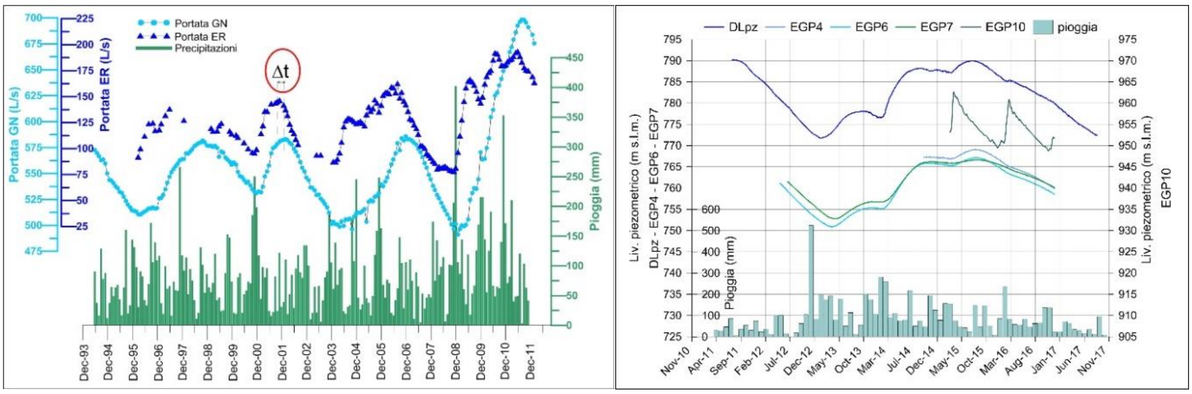

Fig. 2.3 - Monthly flow rates of GN and ER springs compared with the monthly rainfall of the Monte Amiata area (left); evolution of rainfall and piezometric level registered at piezometer DLpz and piezometers of recent construction (right). Δt is the recurrent temporal shift between maximums or minimums of GN spring with respect to those of ER. The rainfall values are achieved by averaging the several stations distributed over the Monte Amiata (from Doveri & Menichini, 2017). See Fig. 2.2 for the location of rainfall stations, piezometers and springs.

Furthermore, they confirmed the pluriannual cycles of increase-decrease of groundwater levels and flow rates, as well as the velocity of about 50 m/d, already calculated by Doveri et al. (2012), regarding the downstream propagation of hydraulic head variations (or flow rate variations) in the aquifer. These results underline the importance of the monitoring activities that have been enhanced during last years, and that should be continued, and possibly further reinforced. This aspect is very important given the strategic role of the Monte Amiata aquifer, which has to be protected and managed in a suitable way, taking also into account the climate trend that the Tuscan region is experiencing (Doveri et al., 2018a). From this point of view the Monte Amiata aquifer can result one of the more sensitive, because of the structural features of the ensemble aquifer-substratum, and the mechanisms and timing of recharge, thus requiring attention and a significant increase of the hydrogeological knowledge.

Geochemical data used in the present report are a compendium of published and unpublished chemical analyses of groundwater samples. Sources are from: (i) published papers in national and international journals (Gambardella et al., 2005; Frondini et. al., 2009; Tassi et al., 2009; Cerrina Feroni et al., 2009; VV. AA. 2010; Doveri et al., 2012; Vaselli et al., 2017); (ii) unpublished data-set kindly provided by "Acquedotto Fiora S.p.A." (Integrated Urban Water Management Company) and (iii) unpublished data-set by the regional network S.I.R.A. (Regional Environmental Information System) that can be downloaded at http://sira.arpat.toscana.it/sira/acqua.php. Groundwater sampling sites (springs and wells) are plotted in Fig. 2.4.

A total of 257 chemical analyses of groundwater discharging in and around the Mt. Amiata were considered in the present report (supplementary material). The chemical data are mainly related to groundwater flowing within the volcanic sequence of the Mt. Amiata. In minor part they regard the local groundwater hosted in the hydrogeological unit n. 2 of Fig. 2.1 and the deep hydrothermal aquifers (i.e. regional evaporitic-carbonate reservoir), well characterized by waters with Ca(Mg)-SO_4-HCO_3 facies and temperature between 20 and 50 °C (Fig. 2.4).

The quality of the available geochemical data was first checked by means of charge balance between cations and anions (i.e. difference < 10% confirms the analytical precision of data). The major ion chemistry showed that anions are mostly represented by HCO_3 (~96%; calculated as proportion of the total of 257 water samples), whereas SO_4 only accounts for ~4% and Cl is always present in subordinate relative amounts. Cations are dominated by (Na+K) and Ca, constituting ~50 and ~49 % of the total samples, respectively, whereas Mg is clustering around ~1 %.

An initial assessment of the chemical composition is obtained by considering the Cl-SO_4-HCO_3 (Fig. 2.5a) and (Na + K)-Ca -Mg (Fig. 2.5b) triangular plots, and the Langelier-Ludwig diagram (Fig. 2.6). In the Cl-SO_4-HCO_3 plot, setting aside 18 samples that fall in the SO_4 field, all the samples are situated in the HCO_3 field. The main cations triangular diagram shows that the water samples distribute in the Na+K and Ca fields, whereas Mg is always present in subordinate relative amounts. Similar consideration are depicted by the square diagram, which shows trends from Ca(+Mg)-HCO_3-SO_4 to (Na+K)-HCO_3-SO_4 facies.

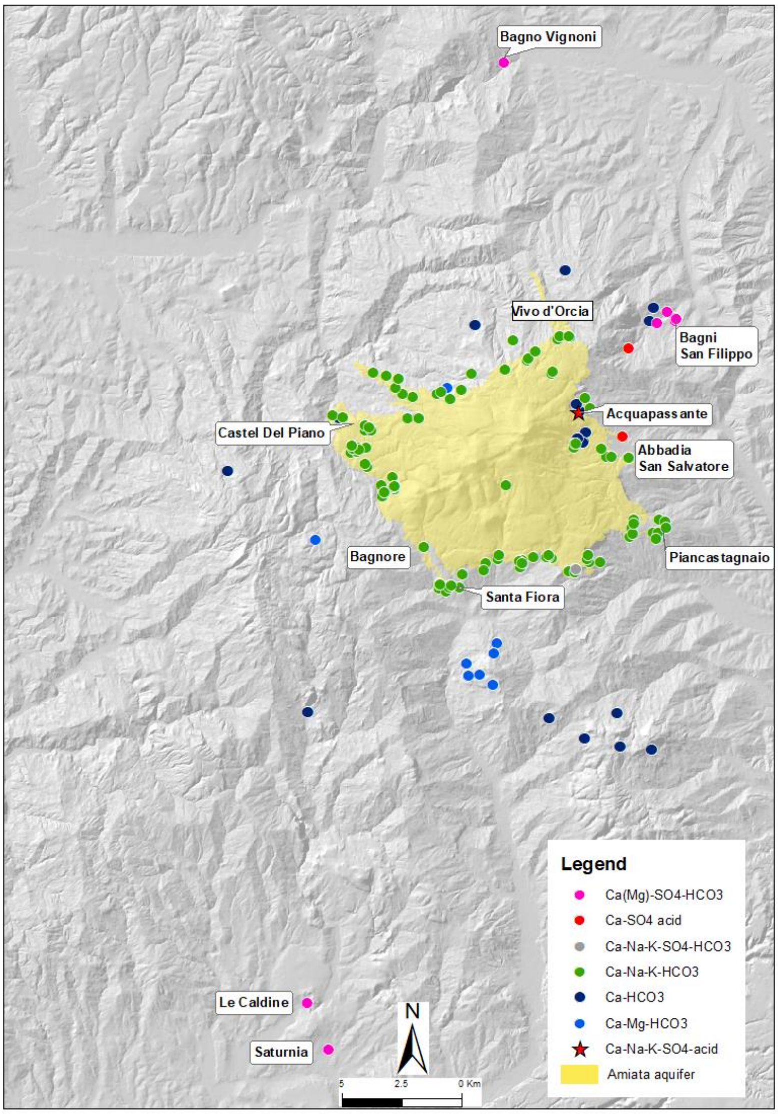

Fig. 2.4 - Sampling sites and chemical composition map for groundwater of the Mt. Amiata area.

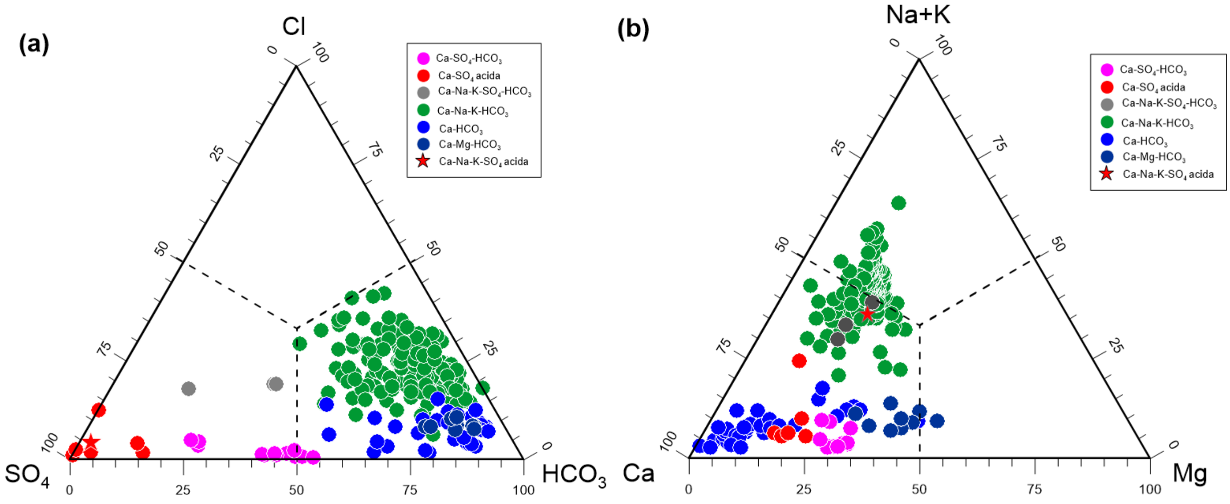

Fig. 2.5 - (a) Cl-SO_4-HCO_3 and (b) Ca-Mg-(Na+K) triangular diagrams for groundwater of the Mt. Amiata area.

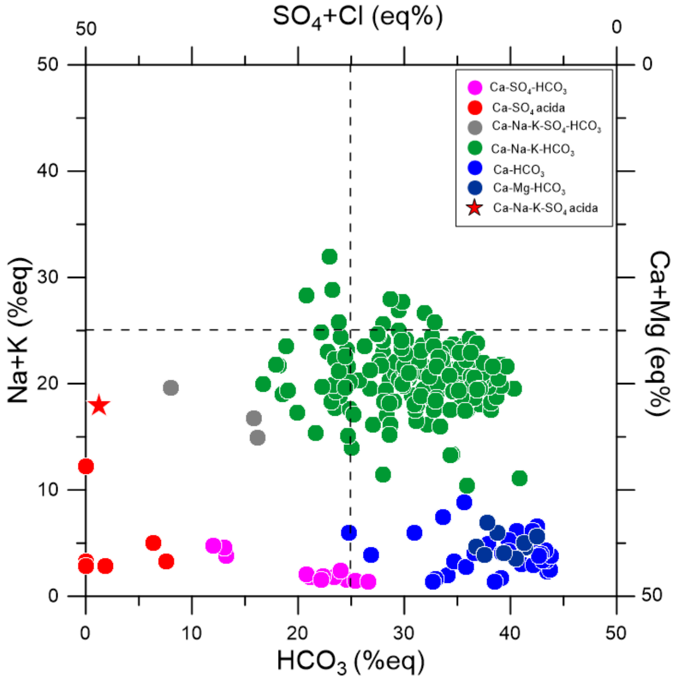

Fig. 2.6 - Langelier-Ludwig square diagram for groundwater of the Mt. Amiata area.

Another useful parameter for water classification is Total Ionic Salinity (TIS) that is the sum of the concentrations of major anions and cations (in meq/L). Iso-TIS lines are drawn in the correlation graph of HCO_3 vs. SO_4+Cl (Fig. 2.7), in which most waters are found between the iso-TIS lines 2 and 10 meq/L, whereas acid (Galleria Italia, Rondinaia and Acquapassante) and thermal waters (Bollore, Terme, Fosso Bianco) are characterized by higher TIS, ranging from 20 to 30 meq/L and 55-125 meq/L, respectively.

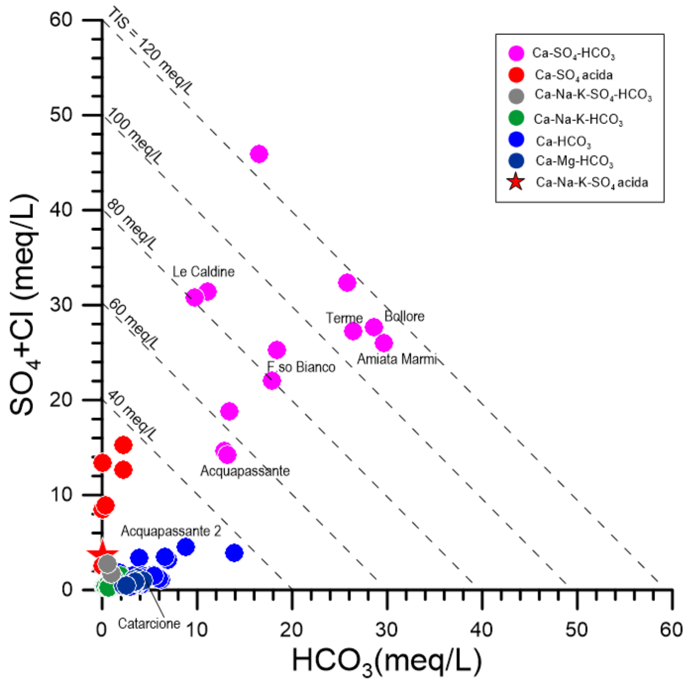

Fig. 2.7 - Salinity plot for groundwater of the Mt. Amiata area.

According to these plots, it is possible to distinguish five groups of waters with different compositions reflecting the rock type and the main geochemical processes characterizing the aquifers of the Mt. Amiata area (Lelli, 2017):

(i) Ca-Na-K-HCO_3 facies. It consists of 194 sample waters (springs and wells) with low salinity (SIT = 1-7 meq/L), produced by interaction of meteoric waters with volcanic rocks of the Mt. Amiata aquifer system. The chemical compositions of this group is characterized by (Na+K)/Mg ratio that overlaps with those of local volcanic rocks (Gambardella et al., 2005 and references therein);

(ii) acid-Ca-Na-K-SO_4 and Ca-Na-K-SO_4-HCO_3 facies. They include samples from the Acquapassante acid spring (SIT = ~ 7.5 meq/L; pH = 3.9), Bagnore Forte (SIT = ~ 7 meq/L) and Pietralunga Alta spring (SIT = ~ 5 meq/L). Waters with an acid-Ca-Na-K-SO_4 (pH values from 3.4 to 5.5) composition are generated through adsorption of H_2S-bearing deep gases into a relatively shallow part of the volcanic aquifer, hosting O_2-rich groundwater, followed by O_2-driven oxidation of H_2S to H_2SO_4 (Gambardella et al., 2005; Frondini et al., 2009). Waters with Ca-Na-K-SO_4-HCO_3 composition are presumable due to either mixing of acid-Ca-Na-K-SO_4 and Ca-Na-K-HCO_3 waters or water-rock interaction processes driven, in distinct moments, by H_2CO_3 and H_2SO_4.

(iii) Ca-HCO_3 e Ca-Mg-HCO_3 facies. It is represented by 42 waters characterized by an intermediate salinity (5<SIT<10) with the exceptions of Acquapassante 2 (SIT = 20 meq/L) and Catarcione (SIT = 3.5 meq/). Generally speaking, this group consists of waters circulating into sandstones of the Pietraforte formations of the volcanics substratum (hydrogeological unit n. 2 in Fig. 2.1), and their composition is likely due to dissolution of Ca-rich and Ca-Mg-rich minerals present into sedimentary rocks (calcilutites and calcarenites).

(iv) acid-Ca-SO_4 facies. This group is characterized by samples namely Galleria Italia (SIT ~ 30 meq/L; pH ~ 5), Rondinaia (SIT = 17 meq/L; pH = 4.18), Mammellone (SIT = 17 meq/L; pH = 5.3) and Acquapassante solfurea (SIT = 5 meq/L; pH = 4.8). The chemical composition of the samples reflects dissolution of Mesozoic carbonate-evaporite formations governed by H_2SO_4, which is originated by either oxidative dissolution of pyrite (at Galleria Italia) or O_2-driven oxidation of H_2S (at Rondinaia) (Vaselli et al., 2017, Tassi et al., 2009). A contribution of evaporite sulfate is also likely and should be ascertain through isotope analyses.

(v) Ca-(Mg)-SO_4-HCO_3 facies. It comprises the 12 water samples discharging at Bagni San Filippo thermal area (i.e.Bollore, Terme, Fosso Bianco, Amiata Marmi, Le Caldine and Acquapassante), having relatively high SIT (55-125 meq/L) and pCO_2 (from 0.19 to 1.01 bar). The chemical features of the thermal waters may be due to interactions of water of meteoric origin with Mesozoic carbonate-evaporite formations (e.g. Chiodini et al., 1995; Tassi et al., 2009 and references therein).

The isotopes of hydrogen and oxygen, being components of water molecules, can trace processes that affect the natural water movement. The oxygen and hydrogen isotopic ratios of natural waters (expressed with the δ notation ‰ and referred to V-SMOW) are linearly correlated according to Global Meteoric Water Line (GMWL): δ^2H (or δD) = $8\delta^{18}O + 10$ (Craig,

1961) and Mediterranean Meteoric Water Line (MMWL): $\delta^2H = 8\delta^{18}O + 20$ (Gat et al., 2003), respectively. In Fig. 2.8, isotopic values of δ^2H vs. $\delta^{18}O$ of groundwater of the Mt. Amiata area are drawn with the reference meteoric lines of local and/or regional interest.

The δD and $\delta^{18}O$ values determined by VV. AA. (2010) range from -60.28 to -31.42 ‰ and from -9.82 to -4.89 ‰ (V-SMOW), respectively (supplementary material). Most samples lies between the global meteoric and the Mediterranean meteoric water lines (Fig. 2.8), thus confirming the meteoric origin of groundwater. The a few exceptions showing weak isotopic shifts (Bagni San Filippo Acquapassante, Anna, Amiata Marmi, Fontanile) are representative of local and secondary processes, such as isotopic fractionation for water-rock interaction, gas-groundwater interaction, evaporation.

The ensemble of the springs of the Mt. Amiata aquifer shows an enough wide range of isotopes values (-6.5÷-10.0‰ and -45÷-60‰, for $\delta^{18}O$ e δ^2H, respectively). This is chiefly tied to different average altitude and exposure (seaward, from where most meteoric perturbation arrives, or inland ward) of the recharge areas that feed the respective springs.

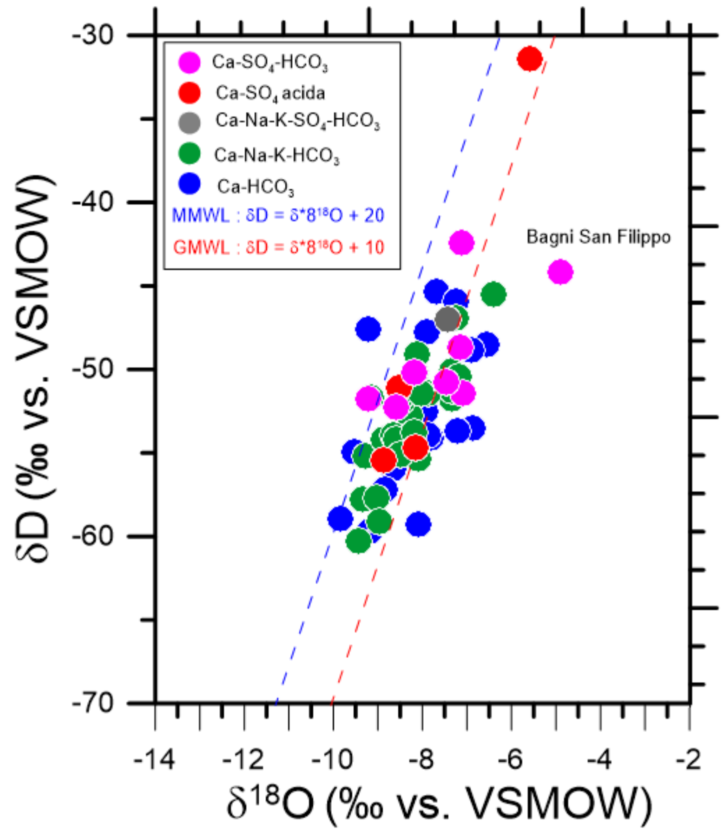

Fig. 2.8 – Hydrogen (as δ^2H‰ V-SMOW) and Oxygen (as $\delta^{18}O$‰ V-SMOW) binary diagram for groundwater of the Mt. Amiata area.

2.2. Synthesis of data and information into the aquifer conceptual model

The ensemble of geological, hydrogeological and geochemical data/information can be compared and summarized into the following main points, thus schematizing the conceptual model of the Mt. Amiata aquifer:

- the volcanics sequence represent the water yielding rocks characterized by values of hydraulic conductivity *K* in the range 5.0E-06 ÷ 4.6E-05 m/s. The aquifer hosted in these rocks is unconfined, as a whole, even if in the inner part of the volcanic edifice a main basal aquifer, in semi-confined conditions, and overlying local perched aquifers are recognizable. The basal substratum of the aquifer is mainly made up by clayey and shaly rocks;
- the recharge in the volcanics aquifer is of the order of 50-55E06 m^3/y and, in first instance, such value is consistent with the total output at springs. Nevertheless, more accurate measurements should be performed for refining these balance evaluations. Most springs are at the contact between volcanics and the substratum of the volcano edifice. Major springs are characterized by flow rate of hundreds L/s. Groundwater flow mainly occurs southwards, given the slope of substratum in this direction;
- groundwater flowing in the Mt. Amiata aquifer are chiefly of the Ca-Na-K-HCO_3 type, thus indicating that the chemistry of these water is essentially affected by their interaction with the volcanics rocks. Only in the NE sector of the volcanic apparatus there are few water points characterized by acid-Ca-Na-K-SO_4, which are likely generated through adsorption of H_2S-bearing deep gases into a relatively shallow part of the aquifer;
- as suggested by water isotopes signature, groundwater hosted in the Mt. Amiata aquifer originate from direct infiltration of meteoric water and it is not affected by secondary isotopic fractionation processes. Hence, the enough wide range of isotopes values showed by the ensemble of springs is linkable to different average altitude and exposure (seaward, from where most meteoric perturbation arrives, or inland ward) of several recharge areas that feed the respective springs. The unsaturated thickness and the hydrodynamic conditions in the aquifer system produce water-infiltration effects on groundwater through pluriannual cycles of increase-decrease of piezometric levels and flow rates.

2.3. Data of monitoring and trends

The aim of the statistical elaboration here performed is to evaluate, in objective terms, the trend over time of groundwater quantity and chemical compounds concentration, thus identifying any statistically significant increase or decrease. Monitoring data for groundwater quantity and quality are available tanks to the activity performed by the water management society (Acquedotto del Fiora SpA), the Hydric Service of the Tuscany Region authority (SIR) and the environmental agency of Tuscany (ARPAT). Furthermore, this study takes also into account data coming from scientific literature. This second group of data have been utilized to evaluate the local chemical background values, whereas data coming from monitoring networks have been used to evidence the presence of temporal trend.

As regards the water chemistry, this report is focused on SO_4, As and B, infact in 2012 ARPAT indicated these chemicals as the most critical variables of the Amiata aquifer. Moreover, to achieve a more complete characterization of the groundwater, from a chemical and physico-chemical point of view, Cl, Conductivity an pH have been added to the data elaboration.

ADOPTED METHODS OF DATA PROCESSING

Evaluation of geochemical background

Probability diagrams are a simple tool of univariate statistics, initially introduced in geochemistry by Tennant and White (1959), Lepeltier (1969) and Bolviken (1971) and subsequently become common, following the works of Sinclair (1974; 1976 1986). The probability graphs allow to recognize the presence of several populations in a given dataset and to divide it into individual populations, starting from the hypothesis that they have a Log-normal, as generally observed for geochemical data, or Normal distribution. This implies that every identified population can be associated with a process or a specific phenomenon that has generated the values belonging to that family. This methodology is generally used to understand how many geochemical processes can have generated the available dataset.

Once the data set has been partitioned into the single populations constituting it, the threshold value can be chosen for each population; this value is usually placed at the 95th percentile or at the UTL (Upper tolerance Limit) value of the population. It can be considered representative of natural processes and not influenced by anthropogenic effects of contamination. Moreover, when trace elements are examined, a certain number of samples is often encountered with concentrations lower than the detection limit, which may be different depending on the source that produced the data. In this study, we chose to consider these data below the detection limit through the Regression on Order Statistics (ROS) methodology.

The processed dataset consists of 258 records distributed over a period of seven years (2003-2009) and it regards chiefly groundwater of the Mt. Amiata aquifer, even though some springs or wells representing surrounding aquifer systems (including thermal systems) are involved for comparison.

Trend analysis

For the chemical data this analysis has been performed on a dataset coming from 10 ARPAT (http://www.arpat.toscana.it/) monitoring stations operating over the period 2002-2016 on springs of the Mt. Amiata aquifer. The following statistical method was adopted:

- Analysis of the frequency distribution of the considered parameters (As, B, Conductivity, pH, SO4 and Cl) through the Shapiro-Wilk and Lilliefors tests;
- Analysis of the presence of potential outlier values, evaluated by Rosner and Dixon tests;

- Analysis of the presence of temporal trends through the non-parametric tests of Theis-Sen with the comparison with Ordinary Last Square (OLS) regression.

As regards the groundwater quantitative data, the flow rate of the GN spring (data from Acquedotto del Fiora SpA) has been analyzed for the period 1990-2017; rainfall and air temperature data from the SIR monitoring network, and referring to the period 1985-2017, have been elaborated as well.

ESTIMATION OF BACKGROUND VALUES

Sulfate (SO_4)

Figure 2.9 shows the Q-Q plot for SO_4, which was elaborated considering all the acquired data and adopting the logarithmic scale on the ordinate axis, because SO_4 data distribute over seven natural logarithm units. Following the Sinclair's approach, the cumulative curve was partitioned in four individual populations, which are composed by 47, 166, 283 and 139 entries, respectively. Figure 2.10 shows the location of the identified populations, whereas the main statistical parameters of these four individual populations are reported in Tab. 2.1, where is also reported the UTL (Upper Tollerance Limit) assumed as threshold value for each single population. According to USEPA (United States Environmental Protection Agency), UTL of the population characterized by lower values (population 4) can be considered as local background threshold limit.

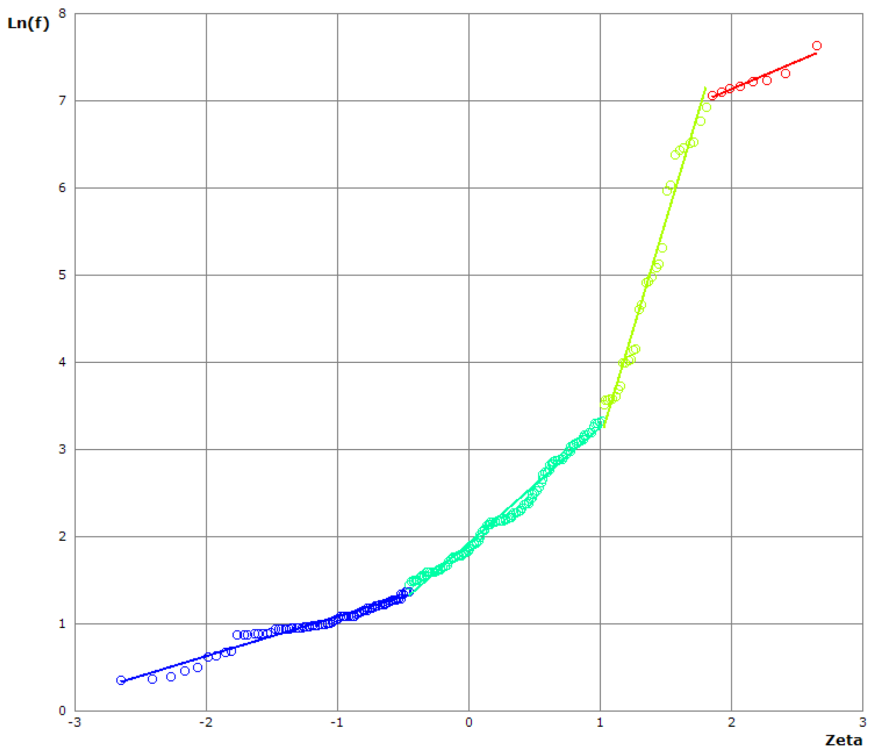

Figure 2.9- Q-Q plot for SO_4 data of the whole dataset.

Population	N	Mean	Median	Min	Max	Std. Dev.	Skewness	Kurtosis	UTL
1	4	1427	1345	1187	2097	289.9	2.155	5.15	2097
2	31	252	107	33.81	1037	292	1.34	0.592	1037
3	140	10.7	8.865	3.87	28.16	6.53	1.12	0.159	27.4
4	77	2.84	2.86	1.45	3.67	0.55	-0.67	0.172	3.66

Table 2.1 - Main statistical parameters for the four individual populations of SO4, recognized using the Sinclair's partitioning procedure

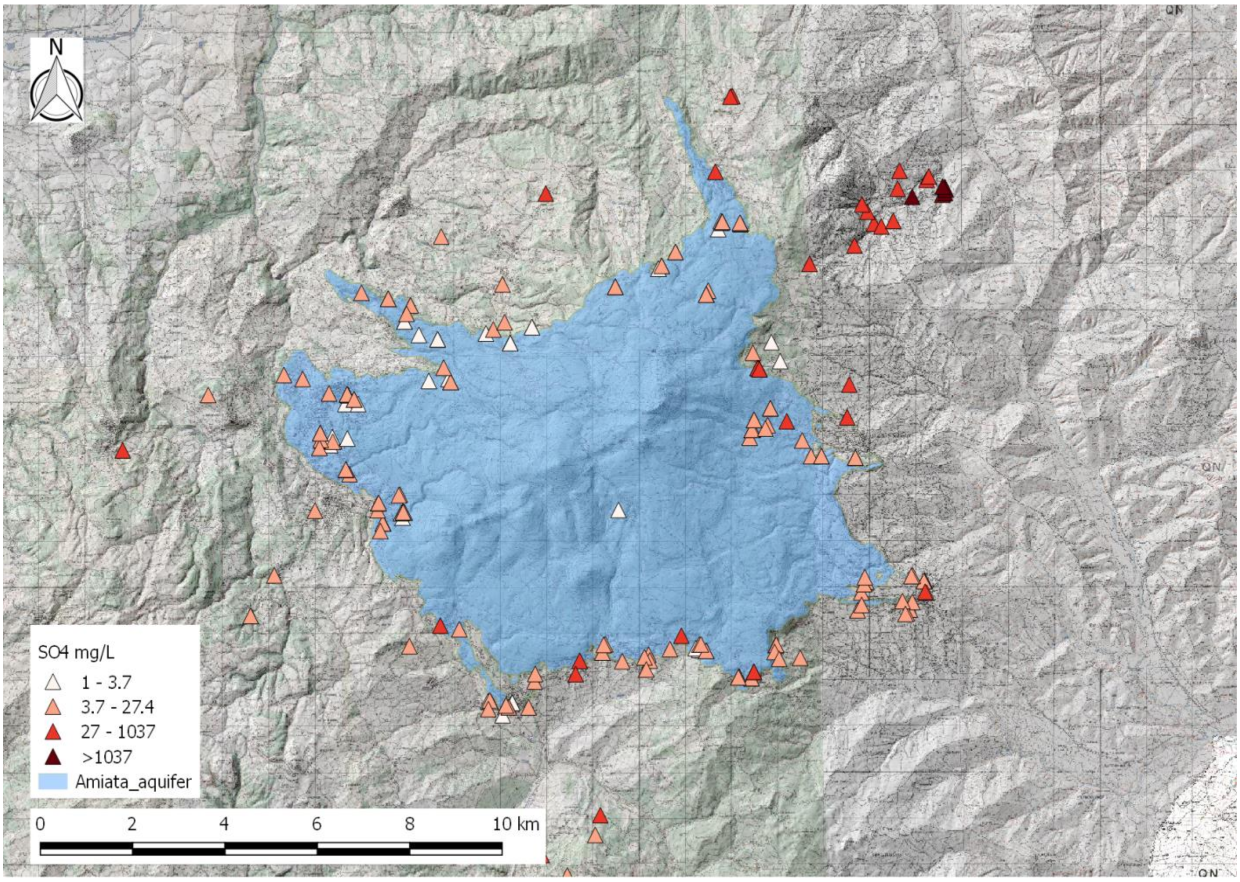

Figure 2.10 - Location of the four populations identify for the SO_4 concentration.

Boron (B)

The Q-Q plots of B is shown in Fig. 2.11. The diagram shows the presence of two different populations. In this case, the UTL limit of lower population is set at 64.42 μg/L.

Figure 2.12 shows the location of the identified populations, whereas the main statistical parameters are reported in Tab. 2.2.

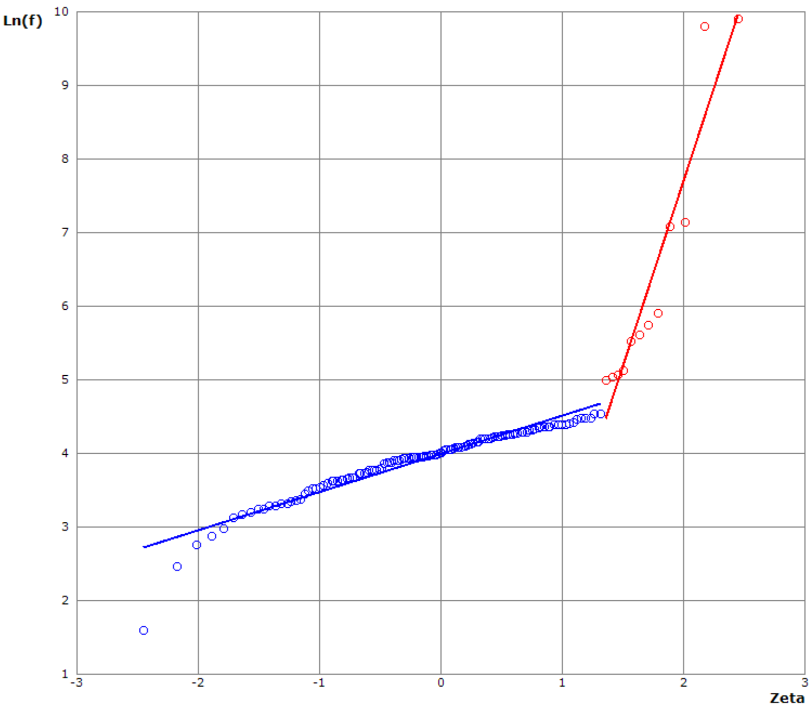

Fig. 2.11 - Q-Q plot for B, based on the whole dataset

Population	N	Mean	Median	Min	Max	Std. Dev.	Skewness	Kurtosis	UTL
1	50	918.3	80	67.81	20188	3805	4.829	22.37	18443
2	86	44.43	46.87	5	67.74	13.78	-0.577	-0.271	64.42

Table 2.2 -Main statistical parameters for the two individual populations of B, recognized using the Sinclair's partitioning procedure

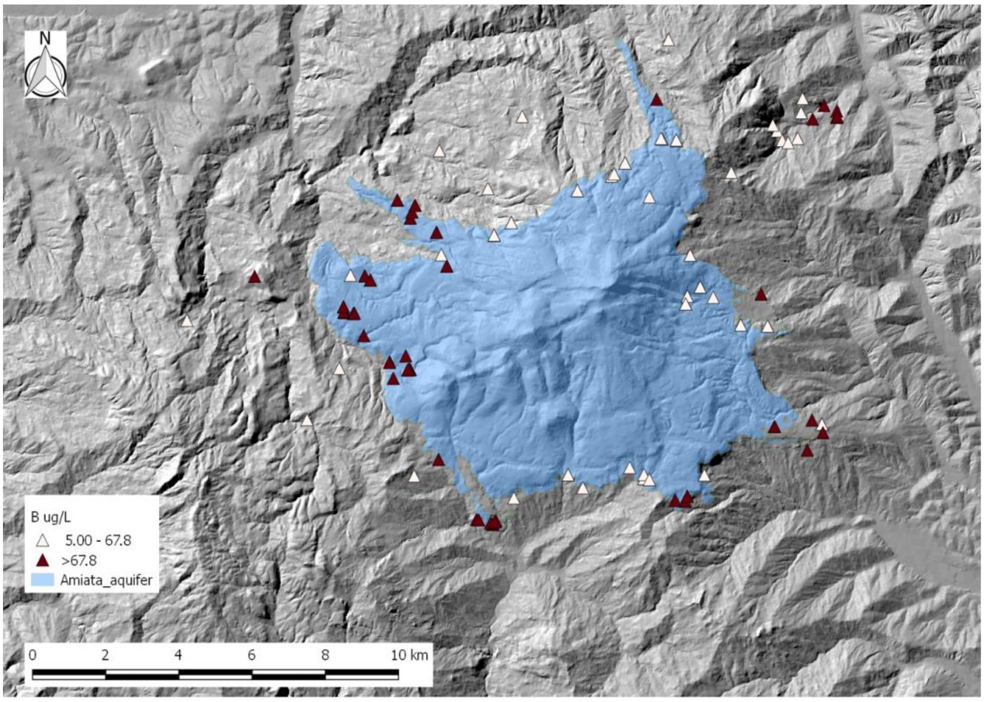

Figure2.12 - Location of the two populations identify in the B concentration.

Chloride (Cl)

Figure 2.13 shows the QQ-plot of chloride concentration regarding the whole dataset. Three higher values and five lower values have been verified to be outliers, so they have been removed from the dataset for evaluating the statistical characteristic of measured data. The new QQ-plot obtained in Fig. 2.14 shows the presence of two populations, whose points are distributed on the territory as in Fig. 2.15. Referring to groundwater of the Mt. Amiata aquifer, it should be noted as the population with higher Cl concentration prevails on the side of the volcanic apparatus seaward exposed (the S-W one), thus pointing out the very likely influence of the sea-salt spray on the quality of infiltrating waters. The lower threshold limit (UTL) is set at 9.1 mg/L (Tab. 2.3).

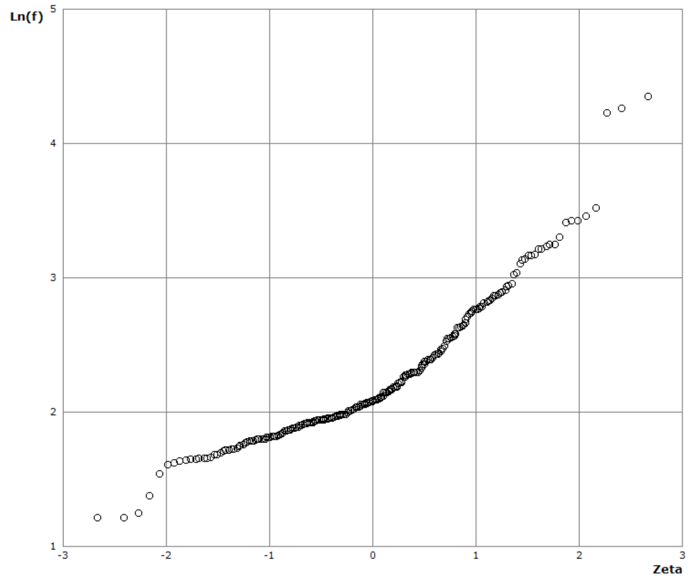

Fig. 2.13 - QQ-plot of Chloride considering the whole available data.

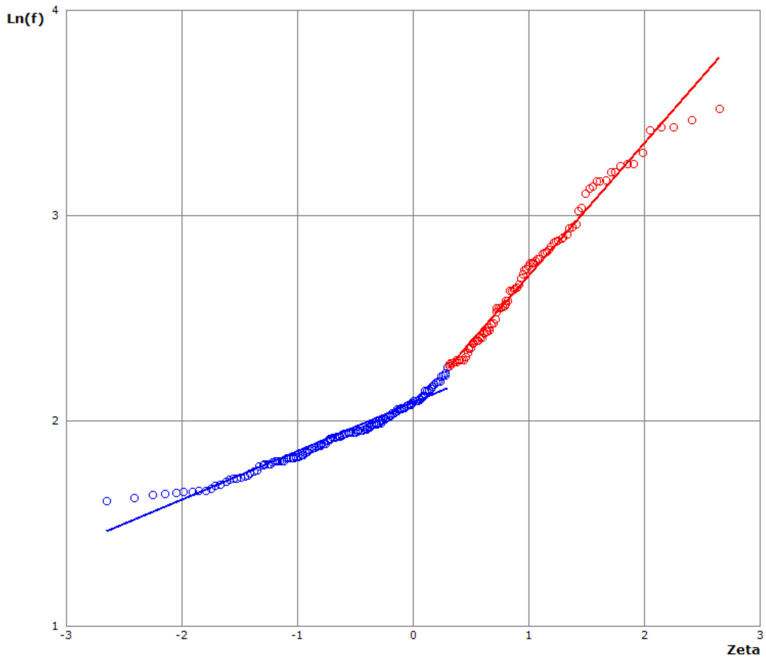

Fig. 2.14 - QQ-plot of chloride excluding outlier values.

Population	N	Mean	Median	Min	Max	Std. Dev.	Skewness	Kurtosis	UTL
1	95	15.85	14.08	9.69	34.02	6.03	1.19	0.72	31
2	154	7.1	7.04	5.02	9.66	1.1	0.16	-0.68	9.146

Tab. 2.3 - Main statistical parameters for the two individual populations of Cl, recognized using the Sinclair's partitioning procedure

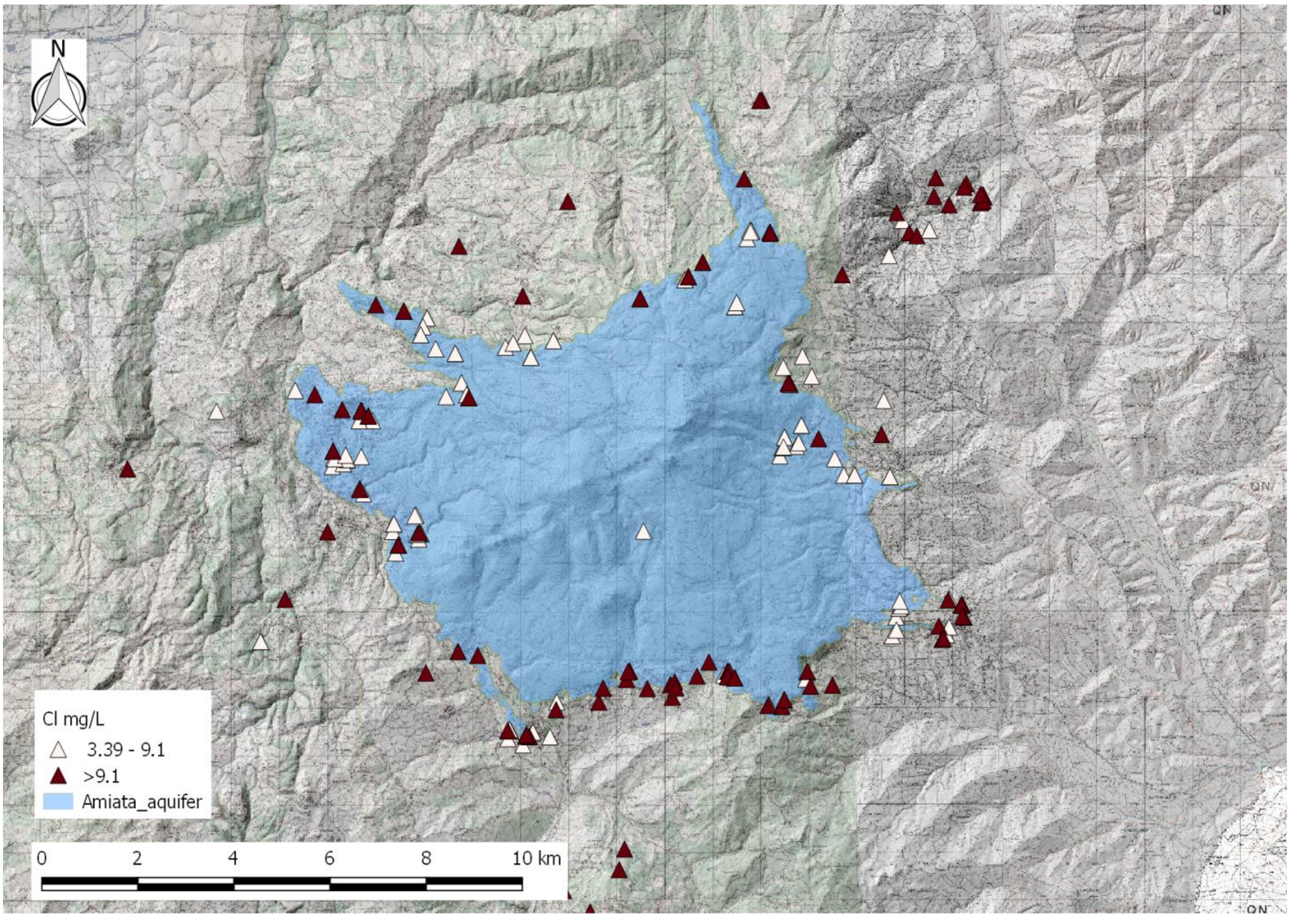

Fig. 2.15 - Location of the two population identify for the Cl concentration.

Electrical Conductivity (EC)

Figure 2.16 shows the QQ-plot related to EC values. There are three population with higher values (10 in total) pertaining to hydrothermal springs. The UTL value of lower population is 138.4 µS/cm. Figure 2.17 shows the location of the dentified populations, whereas the statistical parameters are in Tab. 2.4.

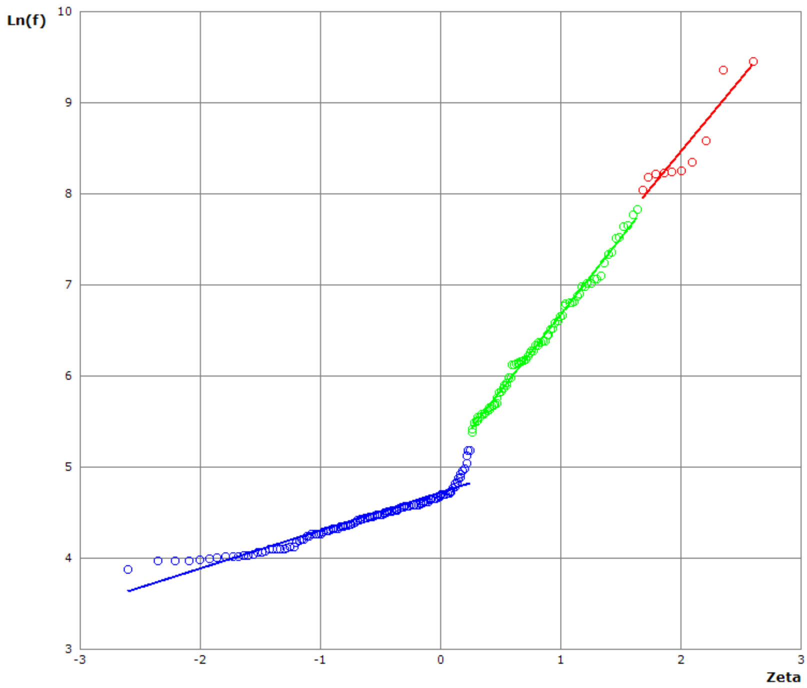

Fig. 2.16 - QQ-plot of EC., considering the whole dataset.

Population	N	Mean	Median	Min	Max	Std. Dev.	Skewness	Kurtosis	UTL
1	10	5642	3860	3130	12950	1140	1.69	1.33	12950
2	75	676.9	523	220	2120	53	1.89	0.68	1853
3	130	90	88.85	49.1	180	23	1.85	0.29	138.4

Tab. 2.4 - Main statistical parameters for the three individual populations of EC, recognized using the Sinclair's partitioning procedure

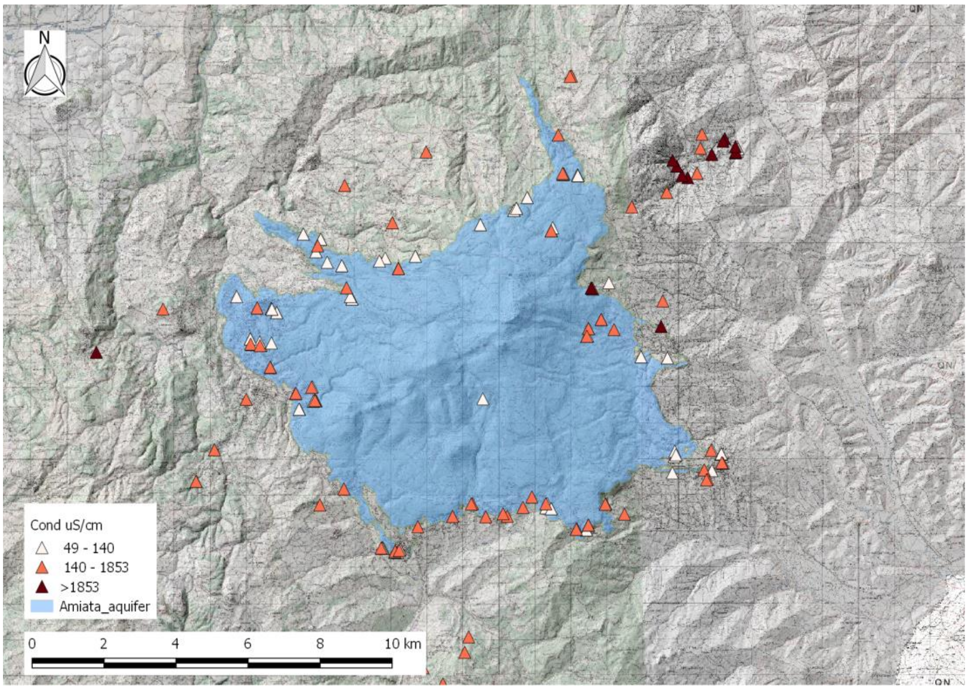

Fig. 2.17 - Location of the three population identify for the EC values.

pH

The QQ-plot of pH (Fig. 2.18) shows the presence of two population. Population 1 refers to already mentioned hydrothermal springs. Diagrams also shows the presence of outlier values (9.02), this value has been excluded from the evaluation of the main statistical parameters resumend in Tab. 2.5. Fig. 2.19 - Location of the two population identify for the pH values.Figure 2.19 shows as the points belonging to the identified populations distribute on the territory.

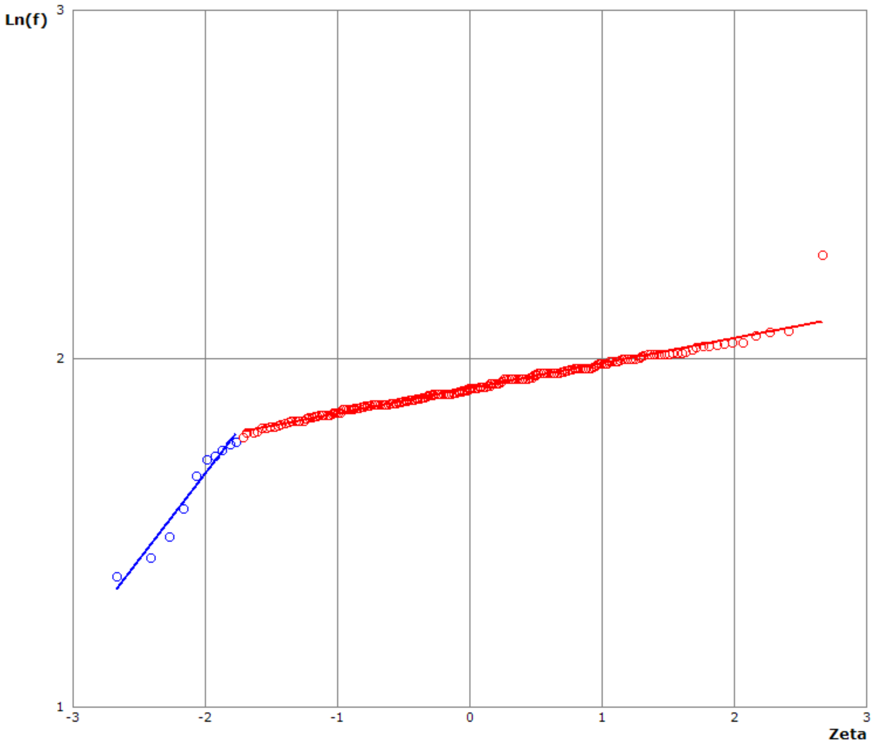

Fig. 2.18 - QQ-plot of pH considering the whole dataset.

Population	N	Mean	Median	Min	Max	Std. Dev.	Skewness	Kurtosis	UTL
1	10	5.117	5.42	3.96	5.83	0.708	-0.634	-1.35	7.18
2	246	6.846	6.8	5.92	8.01	0.427	0.254	-0.404	7.6

Tab. 2.5 - Main statistical parameters for the two individual populations of pH, recognized using the Sinclair's partitioning procedure

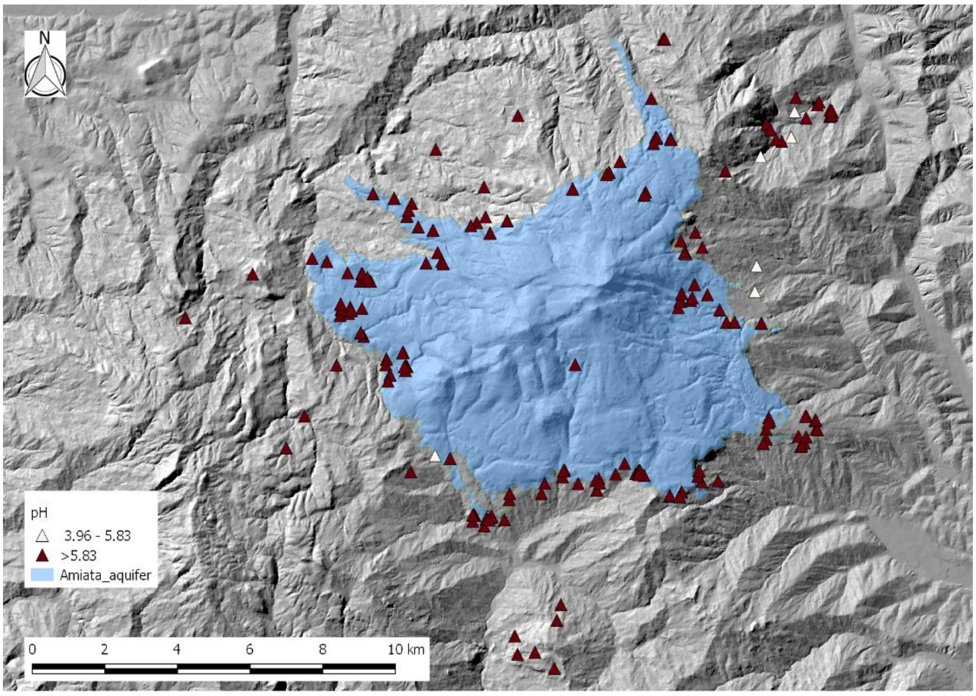

Fig. 2.19 - Location of the two population identify for the pH values.

Arsenic (As)

Arsenic dataset presents two non-detected values, which have been substituted with the half of the detection limit (DL/2; i.e. <4 µg/L ➔ 2 µg/L). QQ-plot of Fig. 2.20 shows the presence of three statistical families, with highest values referring to hydrothermal springs and mine drainage. The UTL threshold limit is set at 0.8 µg/L. However, this limit refers mainly to local shallow groundwater circulating outside of the volcanics aquifer. Taking into account population 2, maybe more representative of the Mt. Amiata aquifer, the UTL threshold is 16.9 µg/L.

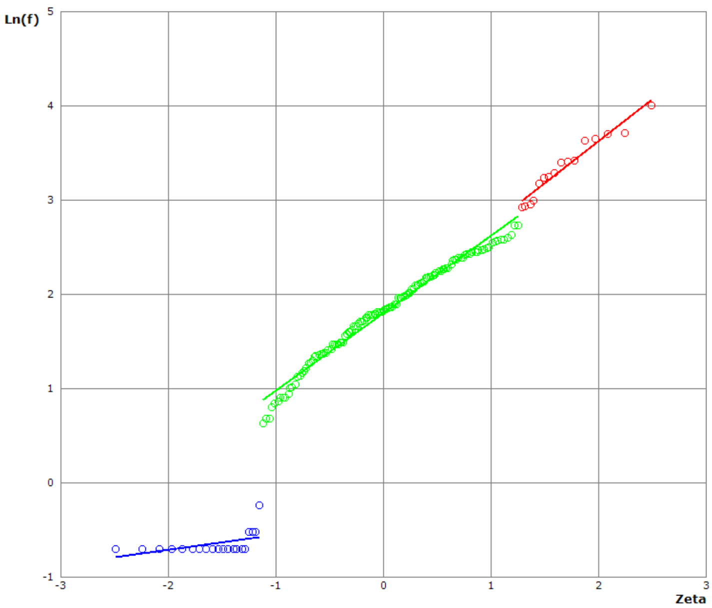

Fig. 2.20 - QQ-plot of As, considering the whole dataset.

Population	N	Mean	Median	Min	Max	Std. Dev.	Skewness	Kurtosis	UTL
1	16	30.38	28.68	18.9	55.2	10.17	0.933	0.722	56.06
2	124	7.13	6.435	1.9	15.6	3.411	0.472	-0.695	16.89
3	20	0.53	0.5	0.5	0.8	0.0733	3.015	9.995	0.8

Tab. 2.6 - Main statistical parameters for the three individual populations of As, recognized using the Sinclair's partitioning procedure.

Fig. 2.19 - Location of the two population identify for the pH values.Figure 2.21 shows the location of the three identified populations.

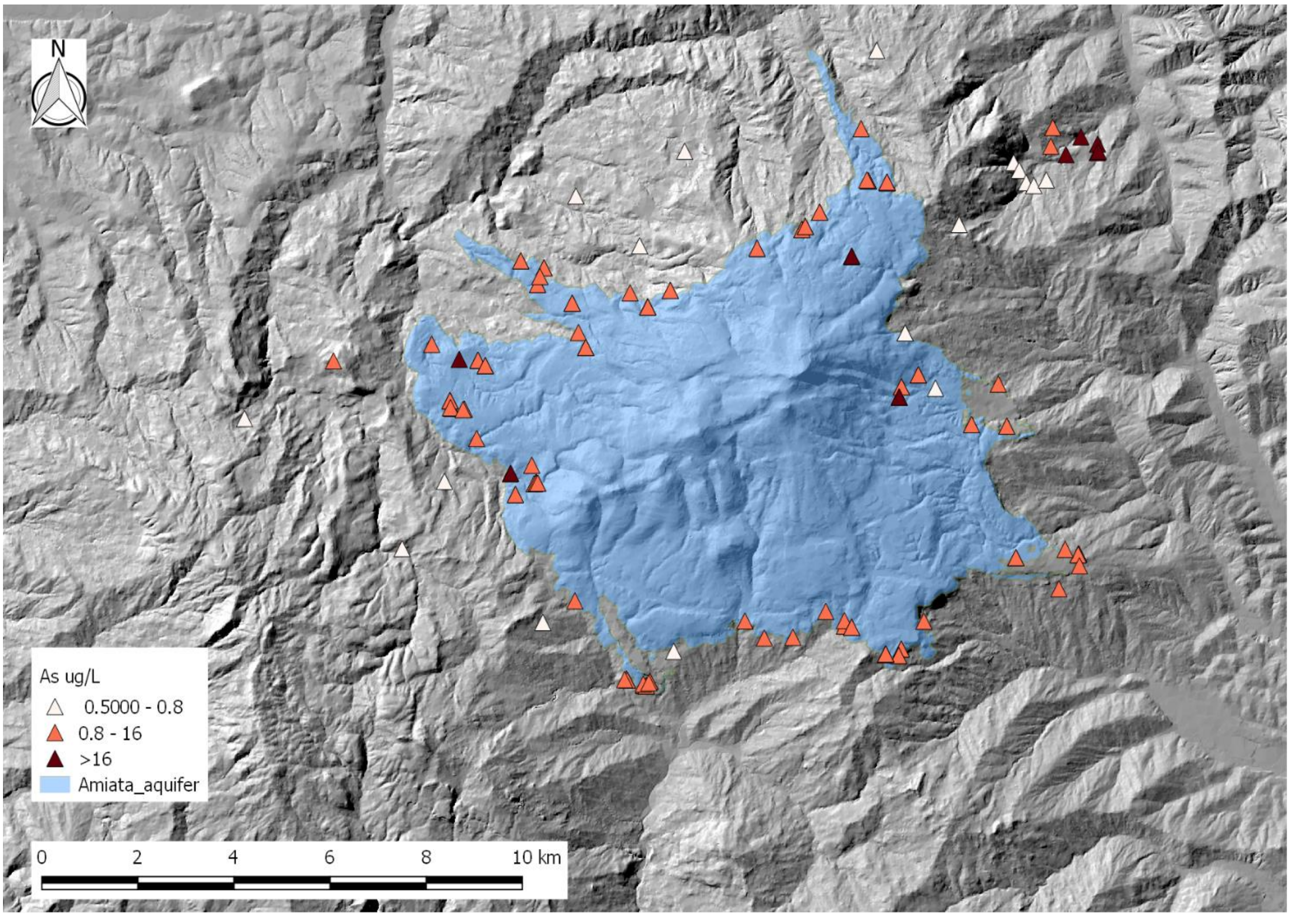

Fig. 2.21 - Location of the three population identify for the As values.

THE MONITORING NETWORK OF HYDRO-CHEMICAL PARAMETERS

On the Mt. Amiata aquifer, the ARPAT monitoring network consists of 10 water collection points (wells and springs). Since 2002 ARPAT monitors the chemistry of groundwater by means of half-yearly sampling. The location of the station is reported in Fig. 2.22, whereas in Tab. 2.7 the station ID and the geographical coordinates have been reported.

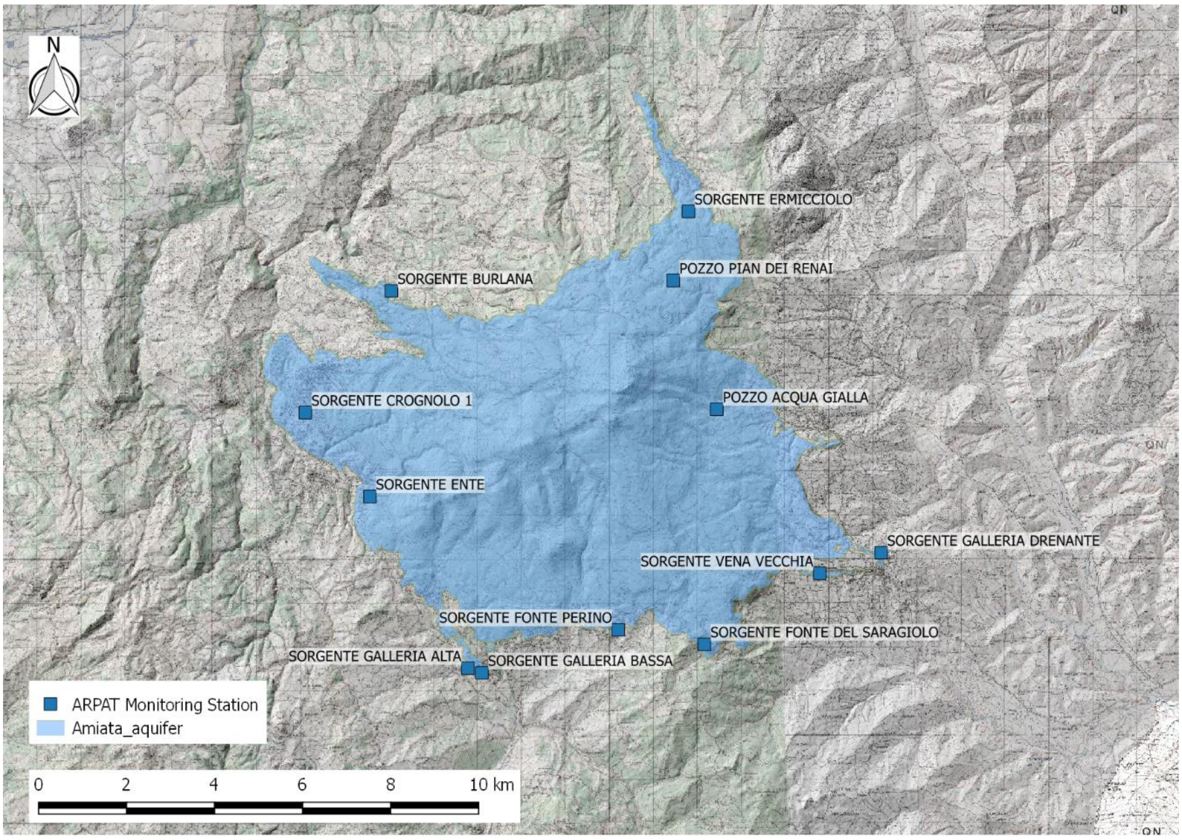

Fig. 2.22 - Location of the ARPAT monitoring stations.

Station_ID	Municipality	station name	GB_E	GB_N	Depth (m)
MAT-S010	ARCIDOSSO	SORGENTE ENTE	1708534	4749224	
MAT-S011	CASTEL DEL PIANO	SORGENTE CROGNOLO 1	1707066	4751134	
MAT-P350	ABBADIA SAN SALVATORE	POZZO PIAN DEI RENAI	1715430	4754140	290
MAT-P596	ABBADIA SAN SALVATORE	POZZO ACQUA GIALLA	1716418	4751209	75
MAT-S020	SANTA FIORA	SORGENTE GALLERIA ALTA	1710758	4745317	
MAT-S021	SEGGIANO	SORGENTE BURLANA	1709023	4753902	
MAT-S045	CASTIGLIONE D'ORCIA	SORGENTE ERMICCIOLO	1715775	4755713	
MAT-S049	PIANCASTAGNAIO	SORGENTE VENA VECCHIA	1718760	4747476	
MAT-S050	PIANCASTAGNAIO	SORGENTE GALLERIA DRENANTE	1720156	4747945	
MAT-S070	SANTA FIORA	SORGENTE FONTE PERINO	1714180	4746193	
MAT-S095	PIANCASTAGNAIO	SORGENTE FONTE DEL SARAGIOLO	1716137	4745861	
MAT-S143	SANTA FIORA	SORGENTE GALLERIA BASSA	1711080	4745212	

Tab. 2.7 - Characteristics and coordinates of the 10 ARPAT monitoring stations.

Following, statistical and trend analyses of As, B, EC, pH, SO_4 and Cl concentrations are performed, also considering the values below DL by means of Rosner test. The applied methodologies are descripted only for the first presented monitoring station, whereas for the other stations the main results are presented.

Acqua Gialla groundwater monitoring station

Parameter	N	Mean	Median	Minimum	Maximum	Std. Dev.	Skewness	Kurtosis
As	48	30.96	26	18.6	154	22.06	4.854	24.21
B	38	56.37	54.5	30	100	12.41	0.901	3.257
EC	47	70.71	71	59.2	83.3	5.576	0.00235	-0.439
pH	46	6.684	6.73	6	7.3	0.311	-0.831	0.595
SO_4	47	9.321	8.8	7	37	4.209	6.438	43.13
Cl	47	5.409	5.4	3.4	7.2	0.531	-0.0269	5.985

Tab, 2.8 - Descriptive statistics for Conductivity, pH, SO4, Cl, B and As of Acqua Gialla monitoring station.

The first step is the searching of outlier value. Each series was submitted to the Rosner test (p = 5%) in order to identify any anomalous values (Outlier). The As presents two outlier (154 e 110 μg/L), the Cl presents two outlier as well (3.4 and 7.2 mg/L), and the SO4 shows one potential outlier (37mg/L). For the pH variable the values equal to 6 has been not considered in order to achieve a parametric distribution. The potential outliers have been eliminated and data were reprocessed starting from the study of distribution.
The Tab. 2.9 shows the main statistical parameters of the investigated variables after the elimination of outlier values.

The results are shown in Fig. 2.23 where the QQ-Plots of each processed parameters are reported. The Shapiro-Wilk test and the Lilliefors test have given the following results: all the parameters follow a Normal distribution, except Cl that follows a Lognormal distribution.

Parameter	N	Mean	Median	Minimum	Maximum	Std. Dev.	Skewness	Kurtosis	Distribution
As	46	26.57	26	18.6	37	3.624	0.533	0.841	Normal
B	37	55.19	54	30	73	10.2	-0.258	0.271	Normal
EC	47	70.71	71	59.2	83.3	5.576	0.00235	-0.439	Normal
pH	41	6.768	6.8	6.33	7.3	0.207	0.222	-0.0583	Normal
SO_4	46	8.72	8.8	7	11	0.844	0.0714	0.118	Normal
Cl	45	5.413	5.4	4.9	6.5	0.361	1.059	1.256	LogNormal

Tab. 2.9 - Descriptive statistics and frequency distribution of EC, pH, SO4, Cl, B and As of Acqua Gialla monitoring station, after elination of outliers values.

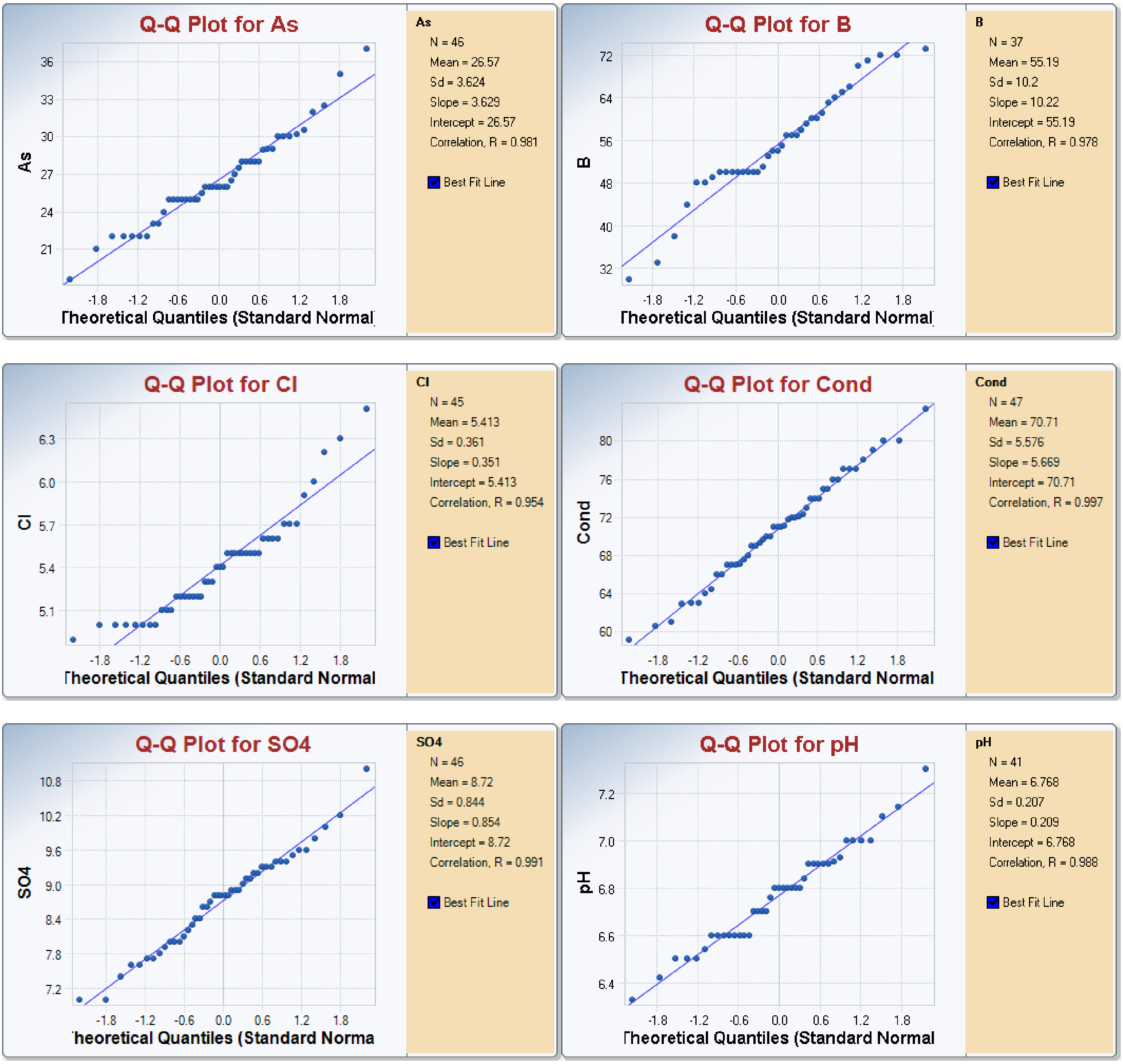

Fig. 2.23 - QQ-Plots of measured As, B, EC, pH, SO4 and Cl in the Acqua Gialla groundwater monitoring station.

The presence of significant trend, at a level of usual significance of 5%, towards the increase or decrease of the concentrations or values measured over time was evaluated both by the non-parametric Theil-Sen statistics and by the Ordinary Last Square (OLS) regression. The results are reported in Fig. 2.24 and in Tab. 2.10.

Fig. 2.24 - Time series of the investigated parameters. The dashed red line refers to Theil-Sen test, while the blue line refers to OLS Regression.

Variable	**OLS Regression**		**Theil-Sen**		**Trend**
	Slope	***Intercept***	***Slope***	***Intercept***	
As	-0.44	916.4	-0.52	1069	Decreasing
B	0.26	474.6	0	54	Insufficient*
EC	-0.35	783.1	-0.37	810	Insufficient*
pH	-0.0051	17.04	0	68	Insufficient*
SO4	-0.14	3018	-0.16	323	Decreasing
Cl	0.01	-16.8	0	5.4	Insufficient*

Tab. 2.10 - Results of trend analysis.

(*) Insufficient evidence to identify a significant trend at the specified level of significance (95%)

Burlana groundwater monitoring station

Parameter	N	Mean	Median	Minimum	Maximum	Std. Dev.	Skewness	Kurtosis
As	41	5.478	5.4	3.7	10.3	1	2.723	13.43
B	40	68.1	68.5	30	120	14.06	0.837	4.728
EC	41	93.92	87	72	173	16.2	3.168	13.76
pH	41	7.051	7	6.5	7.7	0.289	0.231	0.381
SO4	40	3.468	3.45	1.8	5	0.585	-0.0497	1.394
Cl	41	8.041	7.9	6.9	15	1.209	4.918	28.71

Tab. 2.11 - Descriptive statistics for As, B, EC, pH, SO4 and Cl of Burlana monitoring station.

Parameter	N	Mean	Median	Minimum	Maximum	Std. Dev.	Skewness	Kurtosis	Distribution
As	40	5.358	5.4	3.7	7.1	0.644	-0.267	1.999	non parametric
B	38	67.74	68.5	47	91	9.811	0.169	0.396	Normal
EC	40	91.94	87	72	120	10.24	1.073	0.686	non parametric
pH	41	7.051	7	6.5	7.7	0.289	0.231	0.381	non parametric
SO_4	40	3.468	3.45	1.8	5	0.585	-0.0497	1.394	Normal
Cl	40	7.868	7.9	6.9	8.8	0.477	-0.279	-0.156	Normal

Tab. 2.12 - Descriptive statistics and frequency distribution of As, B, EC, pH, SO4 and Cl of Burlana monitoring station, after elination of outliers values.

Variable	OLS Regression		Theil-Sen		Trend
	Slope	*Intercept*	*Slope*	*Intercept*	
As	-0.033	72.13	-0.04	84.97	Insufficient*
B	-0.127	323.8	0	68.5	Insufficient*
EC	-0.668	1436	-0.35	791.4	Insufficient*
pH	0.004	-0.979	0	7	Insufficient*
SO4	0.046	-88.72	0.057	-111.2	Increasing
Cl	0.085	-163.2	0.08	-150.5	Increasing

Tab. 2.13 - Results of trend analysis.

(*) Insufficient evidence to identify a significant trend at the specified level of significance (95%)

Crognolo groundwater monitoring station

Parameter	N	Mean	Median	Minimum	Maximum	Std. Dev.	Skewness	Kurtosis
As	45	11.69	12	1	15	1.973	-3.85	19.98
B	45	63.22	65	25	92	14.3	-0.533	1.135
EC	45	97.17	90	73	206	21.35	3.501	15.39
pH	45	6.943	6.9	6.4	7.8	0.34	1.048	0.864
SO_4	44	3.973	3.6	2.4	14	1.727	4.87	27.52
Cl	45	7.88	7.4	6.6	18	1.959	3.906	17.14

Tab. 2.13 - Descriptive statistics for As, B, EC, pH, SO4 and Cl of Crognolo monitoring station.

Parameter	N	Mean	Median	Minimum	Maximum	Std. Dev.	Skewness	Kurtosis	Distribution
As	44	11.93	12	8.3	15	1.124	-1.039	4.417	non parametric
B	45	63.22	65	25	92	14.3	-0.533	1.135	Normal
EC	41	91.7	89	73	113	7.841	0.55	1.3	non parametric
pH	45	6.943	6.9	6.4	7.8	0.34	1.048	0.864	non parametric
SO_4	41	3.61	3.5	2.4	4.7	0.494	-0.085	0.613	Normal
Cl	41	7.356	7.3	6.6	8.5	0.432	0.535	0.102	Normal

Tab. 2.15 - Descriptive statistics and frequency distribution of As, B, EC, pH, SO4 and Cl of Crognolo monitoring station, after elination of outliers values.

Variable	OLS Regression		Theil-Sen		Trend
	Slope	***Intercept***	***Slope***	***Intercept***	
As	-0.106	225.3	0	12	Insufficient*
B	1.1	-2146	1.02	-1979	Increasing
EC	-0.53	1150	-0.57	1235	Decreasing
pH	-0.024	55.47	-0.0082	23.29	Insufficient*
SO4	-0.013	29.07	-0.02	46.16	Insufficient*
Cl	0.063	-120	0.074	-141.7	Increasing

Tab. 2.16 - Results of trend analysis.

(*) Insufficient evidence to identify a significant trend at the specified level of significance (95%)

Ente groundwater monitoring station

Parameter	N	Mean	Median	Minimum	Maximum	Std. Dev.	Skewness	Kurtosis
As	50	10.96	11	2.3	14	2.136	-2.349	6.476
B	49	76	76	40	110	12.8	-0.286	0.964
EC	50	95.41	94.5	75	125	10.18	0.364	1.127
pH	45	7.359	7.3	6.6	8	0.314	0.208	0.175
SO_4	48	2.985	2.8	1.7	8.7	1.085	3.925	18.21
Cl	49	7.508	7.2	6	14	1.168	4.255	21.34

Tab. 2.17 - Descriptive statistics for As, B, EC, pH, SO4 and Cl of Ente monitoring station.

Tab. 2.18 - Descriptive statistics and frequency distribution of As, B, EC, pH, SO4 and Cl of Ente monitoring station, after elimination of outliers values.

Parameter	N	Mean	Median	Minimum	Maximum	Std. Dev.	Skewness	Kurtosis	Distribution
As	50	10.96	11	2.3	14	2.136	-2.349	6.476	non parametric
B	49	76	76	40	110	12.8	-0.286	0.964	Normal
EC	50	95.41	94.5	75	125	10.18	0.364	1.127	non parametric
pH	45	7.359	7.3	6.6	8	0.314	0.208	0.175	Normal
SO_4	46	2.785	2.8	1.7	4	0.434	0.334	1.789	Normal
Cl	45	7.291	7.2	6.7	8.1	0.34	0.684	-0.0866	LogNormal

Variable	OLS Regression		Theil-Sen		Trend
	Slope	*Intercept*	*Slope*	*Intercept*	
As	-0.098	209	0	11	Insufficient*
B	1.02	-1983	1.1	-2254	Increasing
EC	-0.72	1537	-0.83	1769	Decreasing
pH	-0.013	34.67	0	7.3	Insufficient*
SO4	-0.018	37.98	-0.015	32.81	Insufficient*
Cl	0.016	-24.8	0.02	-33.14	Insufficient*

Tab. 2.19 - Results of trend analysis.

(*) Insufficient evidence to identify a significant trend at the specified level of significance (95%)

Ermicciolo groundwater monitoring station

Parameter	N	Mean	Median	Minimum	Maximum	Std. Dev.	Skewness	Kurtosis
As	49	4.569	4.3	3.2	12	1.278	4.417	24.35
B	40	56.43	56	30	73	9.361	-0.47	0.584
EC	49	88.69	87.4	71.8	154	12.33	3.16	15.83
pH	49	6.84	6.9	6	7.71	0.41	-0.27	0.557
SO_4	48	4.444	3.6	2.7	26	3.611	5.016	28.25
Cl	49	7.441	7.5	5.4	11	1.012	0.997	2.532

Tab. 2.20 - Descriptive statistics for As, B, EC, pH, SO4 and Cl of Ermicciolo monitoring station.

Parameter	N	Mean	Median	Minimum	Maximum	Std. Dev.	Skewness	Kurtosis	Distribution
As	44	4.264	4.3	3.2	5.5	0.43	-0.0652	1.401	Normal
B	40	56.43	56	30	73	9.361	-0.47	0.584	Normal
EC	48	87.33	87.2	71.8	104	7.908	0.27	-0.633	Normal
pH	49	6.84	6.9	6	7.71	0.41	-0.27	0.557	non parametric
SO_4	44	3.6	3.55	2.7	5	0.668	0.6	-0.73	non parametric
Cl	49	7.441	7.5	5.4	11	1.012	0.997	2.532	LogNormal

Tab. 2.21 - Descriptive statistics and frequency distribution of As, B, EC, pH, SO4 and Cl of Ermicciolo monitoring station, after elination of outliers values.

Variable	OLS Regression		Theil-Sen		Trend
	Slope	*Intercept*	*Slope*	*Intercept*	
As	-0.027	57.95	-0.017	37.61	Insufficient*
B	0.0045	47.45	-0.137	331	Insufficient*
EC	-0.753	1601	-0.853	1766	Decreasing
pH	-0.051	110	-0.045	97.7	Decreasing
SO4	-0.09	185	-0.086	175	Decreasing
Cl	0.15	-295	0.132	-258	Increasing

Tab. 2.22 - Results of trend analysis.

(*) Insufficient evidence to identify a significant trend at the specified level of significance (95%)

Galleria Alta groundwater monitoring station (referring to the spring in this report coded as GN)

Parameter	N	Mean	Median	Minimum	Maximum	Std. Dev.	Skewness	Kurtosis
As	49	8.755	9.3	3.8	10	1.504	-2.203	4.238
B	48	70.1	70.5	40	110	13.07	0.236	0.895
EC	49	90.64	87	80	119	7.826	1.756	3.162
pH	50	7.081	7	6.5	8	0.323	0.8	0.66
SO_4	49	3.808	3.5	2.4	13	1.439	5.643	36.15
Cl	50	6.918	6.7	6	9.7	0.808	1.629	2.432

Tab. 2.23 - Descriptive statistics for As, B, EC, pH, SO4 and Cl of Galleria Alta monitoring station.

Parameter	N	Mean	Median	Minimum	Maximum	Std. Dev.	Skewness	Kurtosis	Distribution
As	49	8.755	9.3	3.8	10	1.504	-2.203	4.238	non parametric
B	48	70.1	70.5	40	110	13.07	0.236	0.895	Normal
EC	49	90.64	87	80	119	7.826	1.756	3.162	non parametric
pH	50	7.081	7	6.5	8	0.323	0.8	0.66	non parametric
SO_4	46	3.546	3.5	2.4	4.3	0.412	-0.276	0.51	Normal
Cl	50	6.918	6.7	6	9.7	0.808	1.629	2.432	LogNormal

Tab. 2.24 -. Descriptive statistics and frequency distribution of As, B, EC, pH, SO4 and Cl of Galleria Alta monitoring station, after elination of outliers values.

Variable	OLS Regression		Theil-Sen		Trend
	Slope	***Intercept***	***Slope***	***Intercept***	
As	-0.112	233	0	9.3	Insufficient*
B	0.3	-529	0.2	-330	Insufficient*
EC	-0.525	1146	-0.34	768	Decreasing
pH	-0.013	33.13	-0.005	17.05	Insufficient*
SO4	0.033	-63.03	0.029	-55.6	Insufficient*
Cl	0.127	-249	0.099	-193	Increasing

Tab. 2.25 - Results of trend analysis.

(*) Insufficient evidence to identify a significant trend at the specified level of significance (95%)

Galleria Bassa groundwater monitoring station

Parameter	N	Mean	Median	Minimum	Maximum	Std. Dev.	Skewness	Kurtosis
As	43	8.605	9	4.7	10	1.097	-1.814	3.368
B	43	71.02	71	40	100	13.11	-0.0834	0.188
EC	42	98.27	96	79	126.1	9.053	0.843	1.675
pH	42	7.023	7.015	6.4	8.1	0.328	0.416	1.883
SO_4	41	4.234	4.2	2.7	5.7	0.599	0.00636	0.256
Cl	43	7.409	7.4	6.1	8.5	0.548	-0.251	0.00132

Tab. 2.26 - Descriptive statistics for As, B, EC, pH, SO4 and Cl of Galleria Bassa monitoring station.

Parameter	N	Mean	Median	Minimum	Maximum	Std. Dev.	Skewness	Kurtosis	Distribution
As	38	8.939	9	7.7	10	0.553	-0.757	0.395	non parametric
B	43	71.02	71	40	100	13.11	-0.0834	0.188	Normal
EC	41	97.59	96	79	119	8.01	0.414	0.869	Normal
pH	41	6.997	7.01	6.4	7.5	0.284	-0.476	-0.095	non parametric
SO_4	41	4.234	4.2	2.7	5.7	0.599	0.00636	0.256	Normal
Cl	43	7.409	7.4	6.1	8.5	0.548	-0.251	0.00132	Normal

Tab. 2.27 - Descriptive statistics and frequency distribution of As, B, EC, pH, SO4 and Cl of Galleria Bassa monitoring station, after elination of outliers values.

Variable	OLS Regression		Theil-Sen		Trend
	Slope	*Intercept*	*Slope*	*Intercept*	
As	0.016	-23.76	0.026	-44.04	Insufficient*
B	0.435	-802	0.47	-876	Insufficient*
EC	-0.479	1062	-0.71	1519	Decreasing
pH	0.022	-37.42	0.011	-14.82	Insufficient*
SO4	0.031	-57.9	0.0318	-59.68	Insufficient*
Cl	0.091	-175	0.097	-188	Increasing

Table 1. Results of trend analysis.

(*) Insufficient evidence to identify a significant trend at the specified level of significance (95%)

Galleria Drenante groundwater monitoring station

Parameter	N	Mean	Median	Minimum	Maximum	Std. Dev.	Skewness	Kurtosis
As	48	7.894	7.65	6.1	14.4	1.531	3.023	11.07
B	38	66.29	67	40	90	9.577	-0.176	1.086
EC	48	127.7	123.7	96.1	230	23.65	2.201	6.961
pH	47	7.084	7.12	6.6	7.5	0.232	-0.414	-0.627
SO_4	46	8.265	7.8	5.3	19	2.443	2.319	7.64
Cl	46	9.17	9.1	7.3	12	1.043	0.652	0.217

Tab. 2.29 - Descriptive statistics for As, B, EC, pH, SO4 and Cl of Galleria Drenante monitoring station.

Parameter	N	Mean	Median	Minimum	Maximum	Std. Dev.	Skewness	Kurtosis	Distribution
As	46	7.62	7.6	6.1	9.8	0.775	0.422	0.787	Normal
B	38	66.29	67	40	90	9.577	-0.176	1.086	Normal
EC	45	123.1	123	96.1	162.7	14.59	0.64	0.702	Normal
pH	47	7.084	7.12	6.6	7.5	0.232	-0.414	-0.627	Normal
SO_4	46	8.265	7.8	5.3	19	2.443	2.319	7.64	LogNormal
Cl	46	9.17	9.1	7.3	12	1.043	0.652	0.217	Normal

Tab. 2.30 - Descriptive statistics and frequency distribution of As, B, EC, pH, SO4 and Cl of Galleria Drenante monitoring station, after elination of outliers values.

Variable	OLS Regression		Theil-Sen		Trend
	Slope	***Intercept***	***Slope***	***Intercept***	
As	-0.029	66.1	-0.013	33.3	Insufficient*
B	-0.13	328	-0.15	368	Insufficient*
EC	-1.36	2862	-1.51	3168	Decreasing
pH	0.013	-18.83	0.019	-30.91	Insufficient*
SO4	-0.2	414	-0.187	383	Decreasing
Cl	0.036	-62.6	0	9.1	Insufficient*

Tab. 2.31 - Results of trend analysis.

(*) Insufficient evidence to identify a significant trend at the specified level of significance (95%)

Pian dei Renai groundwater monitoring station

Parameter	N	Mean	Median	Minimum	Maximum	Std. Dev.	Skewness	Kurtosis
As	45	11.38	11	3.4	23	3.248	1.002	3.516
B	30	58.57	52.5	33	210	30.21	4.604	23.51
EC	44	99.06	97.55	83	133	9.243	1.185	2.858
pH	44	6.696	6.73	6	7.2	0.328	-0.858	0.328
SO_4	43	12.24	12	3.8	22.4	2.486	0.839	9.426
Cl	43	6.165	6.2	3.6	7.5	0.632	-1.351	5.858

Tab. 2.32 - Descriptive statistics for As, B, EC, pH, SO4 and Cl of Piana dei Renai monitoring station.

Parameter	N	Mean	Median	Minimum	Maximum	Std. Dev.	Skewness	Kurtosis	Distribution
As	44	11.12	11	3.4	18	2.754	0.157	1.68	non parametric
B	29	53.34	52	33	79	9.89	0.364	0.409	Normal
EC	44	99.06	97.55	83	133	9.243	1.185	2.858	Normal
pH	44	6.696	6.73	6	7.2	0.328	-0.858	0.328	non parametric
SO_4	39	12.18	12	11	14.3	0.816	0.809	0.667	non parametric
Cl	42	6.226	6.2	5	7.5	0.494	0.297	0.922	LogNormal

Tab. 2.33 Descriptive statistics and frequency distribution of As, B, EC, pH, SO4 and Cl of Pian dei Renai monitoring station, after elimination of outliers values.

Variable	OLS Regression		Theil-Sen		Trend
	Slope	***Intercept***	***Slope***	***Intercept***	
As	0.096	-8.15	0	11	Insufficient*
B	-0.41	868	-0.23	518	Insufficient*
EC	0.055	-11.13	-0.4	908	Insufficient*
pH	-0.04	89.6	-0.033	73.8	Decreasing
SO4	-0.022	57.04	0	12	Insufficient*
Cl	0.01	-14.26	0.016	-25.1	Insufficient*

Tab. 2.34 Results of trend analysis.

(*) Insufficient evidence to identify a significant trend at the specified level of significance (95%)

Vena Vecchia groundwater monitoring station

Parameter	N	Mean	Median	Minimum	Maximum	Std. Dev.	Skewness	Kurtosis
As	47	7.432	7.4	5.7	11.5	1.052	1.471	4.074
B	38	65.37	64	40	91	10.94	0.0606	0.672
EC	47	105.6	104	92.1	130	8.503	0.707	0.642
pH	47	6.934	6.9	6.5	7.54	0.178	0.847	2.798
SO_4	45	5.896	5.8	3	9.9	1.156	1.226	3.475
Cl	46	7.967	8.1	4.8	10	1.19	-1.286	1.906

Tab. 2.35 - Descriptive statistics for As, B, EC, pH, SO4 and Cl of Vena Vecchia monitoring station.

Parameter	N	Mean	Median	Minimum	Maximum	Std. Dev.	Skewness	Kurtosis	Distribution
As	46	7.343	7.35	5.7	9.6	0.869	0.606	0.816	Normal
B	38	65.37	64	40	91	10.94	0.0606	0.672	Normal
EC	47	105.6	104	92.1	130	8.503	0.707	0.642	Normal
pH	45	6.91	6.9	6.5	7.17	0.139	-0.469	0.511	Normal
SO_4	41	5.739	5.7	4.8	7.4	0.69	0.753	-0.0793	Normal
Cl	41	8.312	8.3	7.1	10	0.671	0.575	0.0631	Normal

Tab. 2.36 - Descriptive statistics and frequency distribution of As, B, EC, pH, SO4 and Cl of Vena Vecchia monitoring station, after elination of outliers values.

Variable	OLS Regression		Theil-Sen		Trend
	Slope	***Intercept***	***Slope***	***Intercept***	
As	-0.059	125	-0.04	90.6	Insufficient*
B	-0.12	311	0	64	Insufficient*
EC	-0.41	940	-0.57	1248	Insufficient*
pH	0.001	4.72	0	6.9	Insufficient*
SO4	-0.052	111	-0.057	120	Decreasing
Cl	0.099	-190	0.11	-205	Increasing

Tab. 2.37 - Results of trend analysis.
(*) Insufficient evidence to identify a significant trend at the specified level of significance (95%)

* * *

The results obtained by the data processing above described can be briefly resumed as follow:

As - the samples belonging to the highest statistical population correspond to the hydrothermal water, anyway there are also high values in the western slope (Fontana I pozzoni and Bagnoli Inferiore e Superiore) and in the eastern slope (Pian dei Renai and Acqua Gialla) of the Mt. Amiata acquifer

B - highest values pertain to thermal manifestation of Bagni San Filippo area. Moreover samples seem to show higher values in the west and south side in respect to north and east slope of the Mt. Amiata aquifer

EC - highest values correspond to hydrotherm springs of Bagni San Filippo. However there are also high values in the eastern side (Acquapassante and Galleria Italia). Moreover, in the southern side tends to prevail values belonging to the second population, while the northern slope shows the prevalence of lower values.

pH – the acid waters (pH>5.8) are located in the Bagni San Filippo area, near Abbadia San Salvatore (Galleria nuova Italia e Galleria Italia), and in the south-west slope (Bagnore Fonte).

SO_4 - highest values correspond to hydrothermal springs of Bagni San Filippo area. The southern and eastern slopes are characterized by the presence of values belonging to medium and medium-high populations, while the northern and western sides are characterized by lower values (population 3 and 4).

Cl – highest values are located far from the Amiata volcano. Nevertheless the southern sector of the aquifer seems to show higher values respect to the northern side.

For what concern the trend analysis of monitoring data, the more significant result concerns the Cl. The main part of groundwater monitored by ARPAT (6 over 10 monitoring stations) show an increasing trend of chloride. Excluding in few cases SO_4 and EC. The other investigated parameters do not show the presence of temporal trend at the 95% level of significance.

QUANTITATIVE ANALYSIS OF WATER RESOURCES

In Fig. 2.25 the monthly values of Mt. Amiata rainfall and GN-spring average flow rate are plotted for the period 1990-2017. The rainfall is accounted as average value over the entire volcanics outcrop, calculated starting from 8 meteo-climatic gauge stations of the Tuscany-SIR (www.sir.toscana.it). The diagram clearly shows the typical plurennial cycles of discharge increase-decrease and different ranges of flow rate values between the period 1990-2009 and the period 2010-2018 as well.

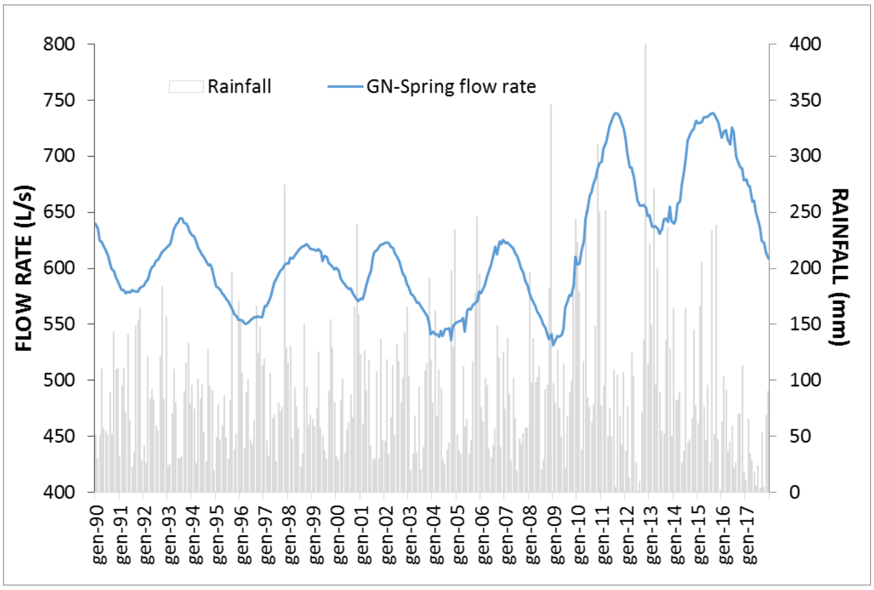

Fig. 2.25 – Monthly data of GN-spring average flow rate and rainfall occurred on the Mt. Amiata aquifer (Flow rate data from Acquedotto del Fiora SpA; Rainfall values achieved elaborating data of several meteo-climatic stations of the SIR, www.sir.toscana.it).

In the later period, the two pick maximum values are nearly 750 L/s, whereas in the former the four cycles show maximum values in the range 625-650 L/s. Also the only one low-flow rate moment observed after 2009 is characterized by significantly higher value respect to those in the previous period (about 650 L/s respect to values in the range 525-575 L/s).

Based on this different hydrodynamic behaviour of the GN spring along the two periods (before and after 2009), a preliminary trend analyses has been performed by using the Theil-Sen test separately over such as sub-period, for both flow rates and rainfall. The results in Fig. 2.26 point out a statistically significant decreasing of flow rate at spring over the period 1990-2009, whereas for the same period there are not sufficient evidences of rainfall trend. On the other hand, for the period 2010-2017 none trend is observed for the discharge of the spring, whereas a significant decreasing trend occurs for the rainfall (Fig. 2.27).

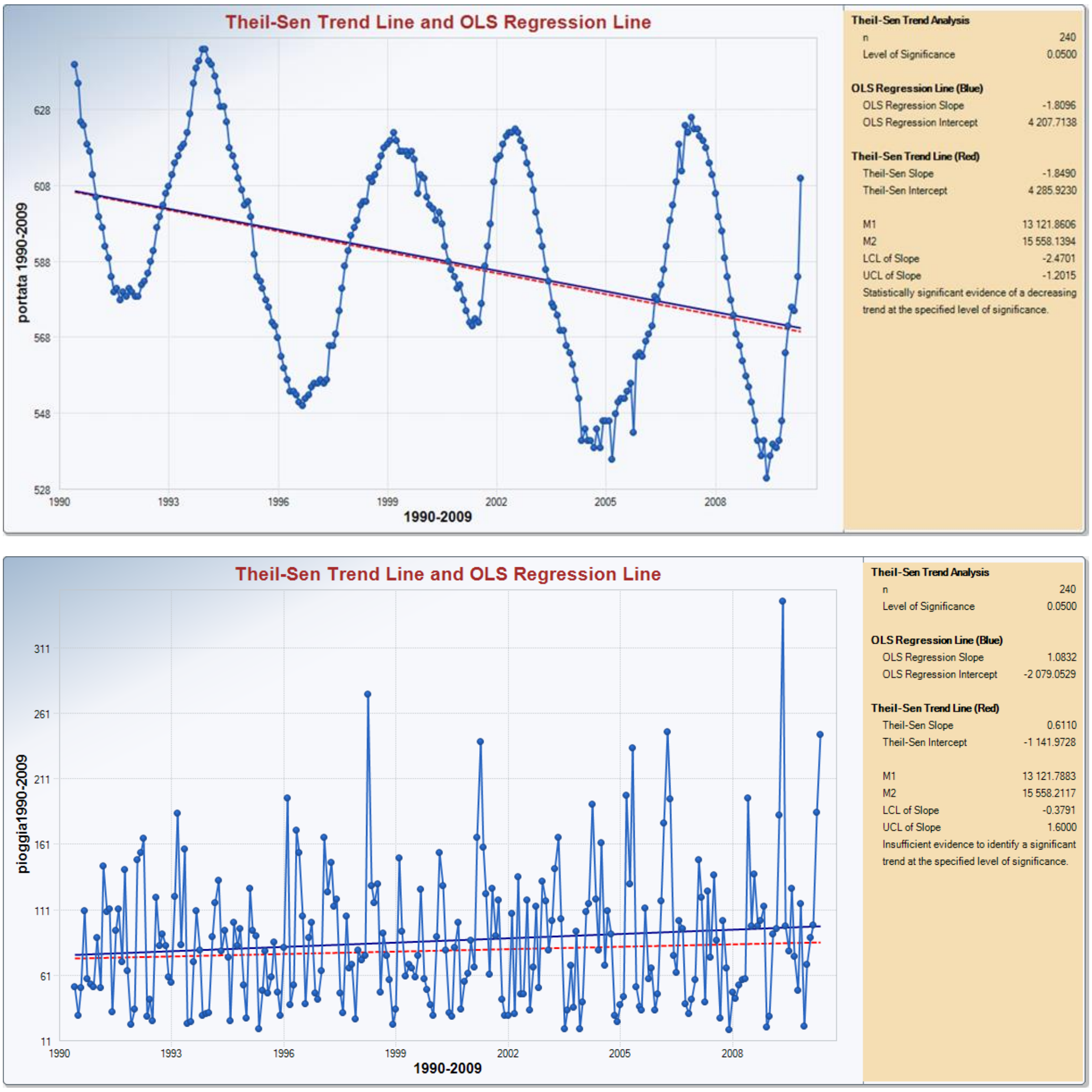

Fig. 2.26 – Time series of monthly rainfall and GN-flow rate over the 1990-2009 period. The dashed red line refers to Theil-Sen test, while the blue line refers to OLS Regression.

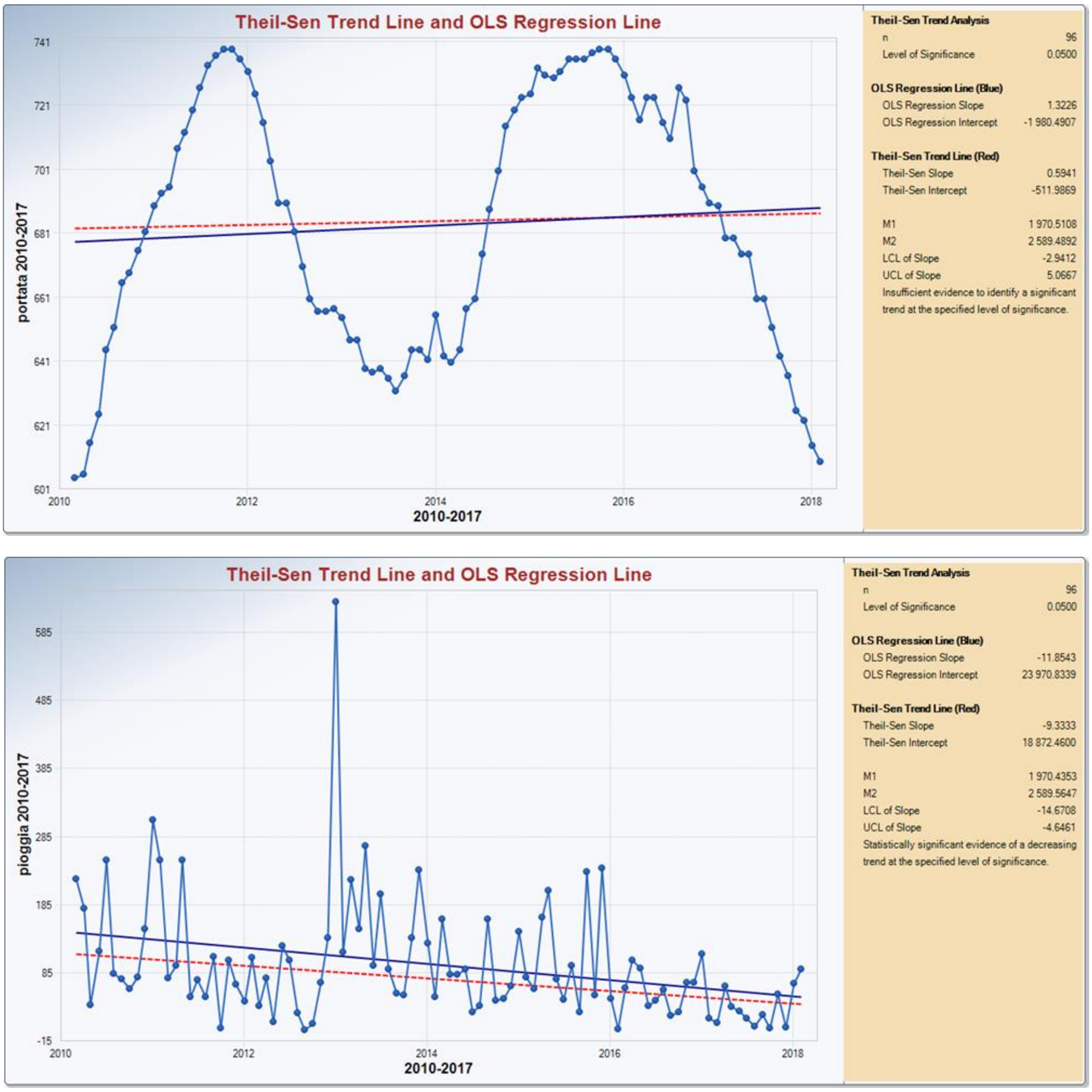

Fig. 2.27 – Time series of monthly rainfall and GN-flow rate over the 2010-2017 period. The dashed red line refers to Theil-Sen test, while the blue line refers to OLS Regression.

After this preliminary analyses none evidence of direct relationship between spring flow rate and rainfall seams to exist. Nevertheless, a more deeply analysis is required by involving other parameters or combination of parameters for verifying the effects of meteo-climatic conditions on groundwater yielding, taking also into account the possible time-lag between “whether events” and aquifer responses. In these terms, the diagram of Fig. 2.28 is propitious, given the significant qualitative relationship that it shows between the discharge evolution and the “24-months moving average” evaluated on the effective rainfall (that for the Mt. Amiata volcano is roughly representative of the infiltration). The latter parameter has been achieved by combining rainfall and temperature into the Thornthwaite & Mather (1955) water balance method. Nevertheless, refinements of the calculation processes will be done for next deliverable, with particular reference to the values of atmospheric temperature to be accounted, given the paucity of dataset on this parameter, both in space and in time.

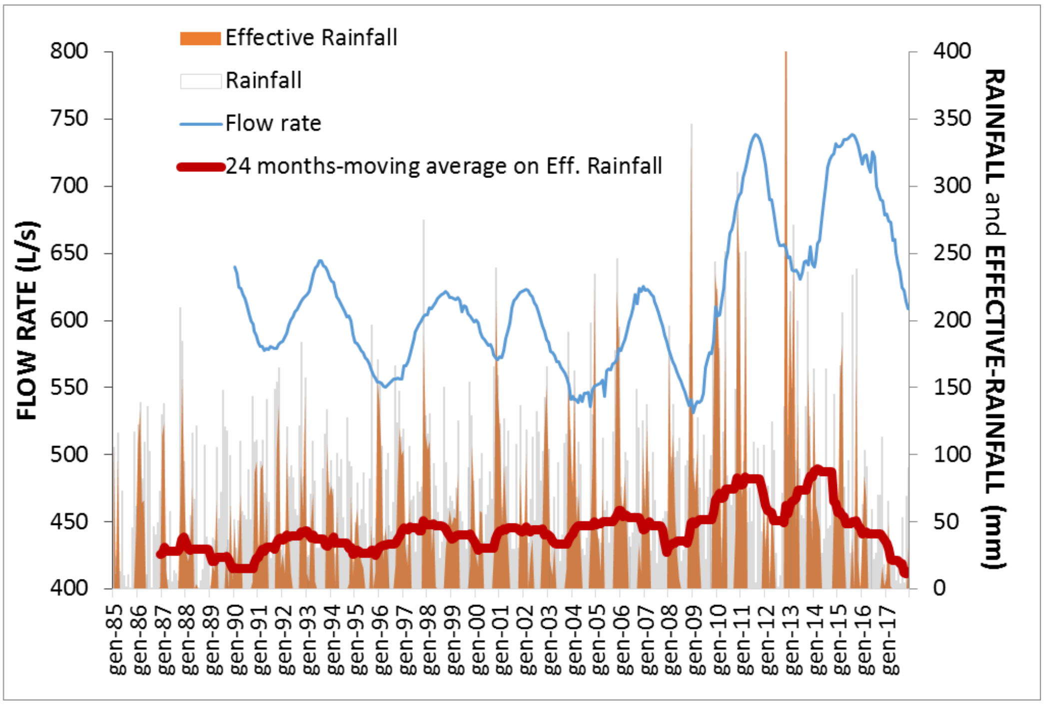

Fig. 2.28 – Time series of monthly rainfall, effective rainfall and GN-flow rate over the 1985-2017 period. A curve of 24 months-moving average on effective rainfall data is also showed.

3. THE APUAN ALPS AQUIFER SYSTEM

3.1. Geological, hydrogeological and geochemical setting

The rocks outcropping in the Apuan Alps area belong to several tectonic-stratigraphic units involved in the Northern Apennine nappe stack (Carmignani & Kligfield, 1990; Conti et al., 1993; Molli & Meccheri, 2012, and references therein). The lower units, which as a whole make up the metamorphic core complex, are the Apuan Alps Unit and the Massa Unit. Overlapping them there are non-metamorphic units, the Tuscan Nappe Unit and Ligurian units, and the Neogene to Quaternary sediments.

The stratigraphic sequence of the Apuan Alps Unit includes a schist-phyllitic basement, and a predominant carbonate sequences aged between upper Triassic and Late Oligocene (Fig. 3.1). The Mesozoic carbonate platform facies have a total thickness varying from 300 to 800 m and consist of dolomite, named "Grezzoni", dolomitic marble and marble (Marmi Dolomitici e Marmi). Above the marble are calcareous schists and meta-limestone with recrystallized layers and nodules of chert (Calcari Selciferi), indicating a transition to a pelagic sedimentation. Cherty limestone is followed by red to green meta-radiolarite (Diaspri and Scisti diasprini). A new horizon of meta-limestones with recrystallized chert (Calcari Selciferi a Entrochi) occurs at the Jurassic-Cretaceous transition and is followed by a gradual transition to sericite-chlorite rich phyllites (Scisti Sericitici), with lenses of calcschists ("Cipollini" marbles). The metamorphic sedimentary sequence ends with Oligocene siliciclastic meta-turbidites, which are named "Pseudomacigno". All these formations have been affected by regional metamorphism of low-grade facies of green schists.

The Massa Unit consists of a continental succession, tectonically reduced to only lower terms, resting on a Palaeozoic basement similar to that of the Apuan Alps Unit. On the metamorphic basement, two short sedimentary cycles succeed. The first cycle begins with lower Triassic continental deposits and siliceous phyllites (Filladi Nere), on which dolomitic marbles (Marmi a Crinoidi) and breccia marble rest. The second cycle is mainly made up by quartz and phyllitic meta-arenite (Filladi Superiori - Ladinian - Carnian), which rests with an erosional contact on the previous cycle deposits.

Apuan Alps and Massa units are tectonically covered by the Tuscan Nappe, which represents the main non-metamorphic unit of Tuscan domain. In the Apuan Alps area, above a horizon of carbonate breccias interposed between metamorphic and non-metamorphic units (usually mapped as "Cavernous" limestone), we find a sequence consisting of carbonate to turbidite formations, Rethian to Upper Oligocene in age, similar to that of the Apuan Alps Unit.

The major faults linked to Plio-Pleistocene extensional tectonic phases regard the non-metamorphic units. Some of these faults enable deep waters to flow to the surface, thus generating a few thermo-mineral springs at the eastern and northern boundaries of the Apuan Alps (Molli et al, 2015). The tectonic unloading of the metamorphic massif (older phase of the Plio-Pleistocene tectonics) was characterized by a general E-W extension. Two main types of brittle deformation developed in the metamorphic core, generating strike-slip and normal faults with small displacements (Molli et al., 2010; Ottria & Molli, 2000; Vaselli et al., 2012). The paucity of a pervasive fracturing pattern within the deep part of metamorphic carbonates promotes the high quality of marble, which is widely quarried for producing ornamental stones, as the world famous Carrara Marble.

The main aquifer system of the Apuan Alps (here after the Apuan Alps aquifer system) is that developed in the metamorphic carbonate sequence of the Apuan Unit (Civita et al., 1991; Piccini et al., 1999; Doveri et al., 2018b and references therein), which is limited by the impervious rocks of the basement at the bottom, and at the top by rocks with medium to low permeability (Fig. 3.1). Dolostones, dolomitic marbles, marbles and cherty metalimestone are arranged into several first-order hydrogeological structures, which are delimited by the contact with the impermeable basement or with clastic sedimentary covers. These structures can host contiguous but hydrogeologically distinct underground drainage systems (Fig. 3.2). In many cases, the drainage system feeds a unique spring. In other cases, the discharge is dispersed over an area in which water outflow occurs in several points or along streams. In all cases, the main springs are located within the major valley incisions at lower altitudes.

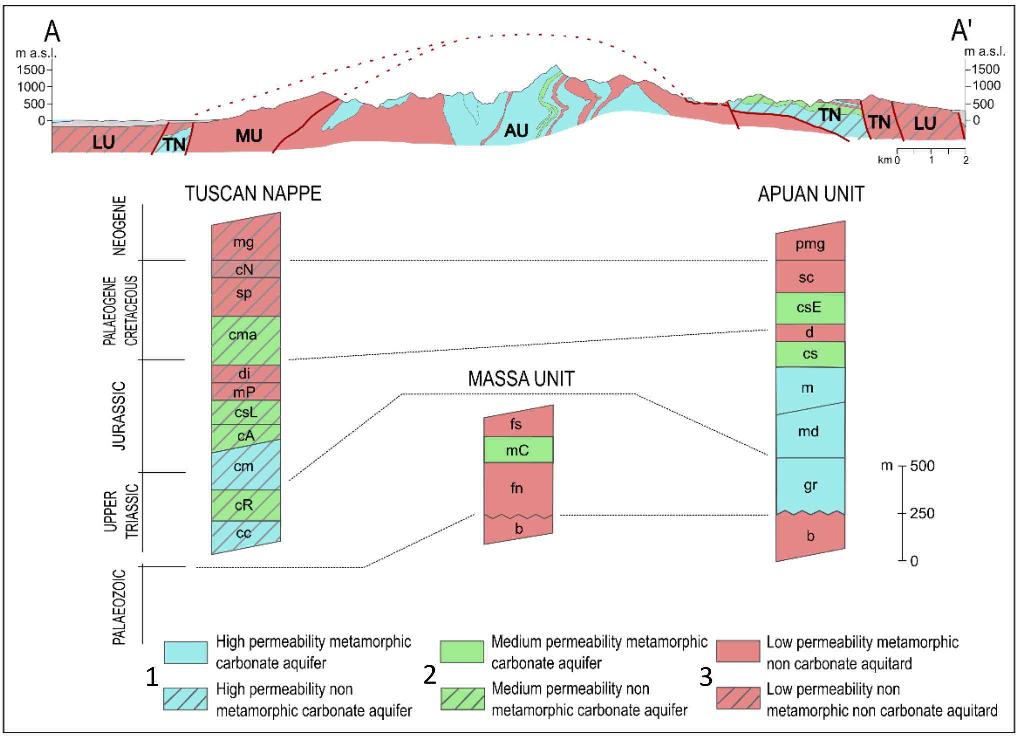

Fig. 3.1 - Simplified hydro-stratigraphic columns of the Apuan Alps, Massa metamorphic units and Tuscan Nappe; thickness of lithostratigraphic units are only indicative (from Doveri et al., 2018b). Permeability grade: 1) carbonate rocks with high permeability with well-developed karst; 2) carbonate rocks with medium permeability due to fracturing and local karst; 3) non-carbonate rocks with low to very low permeability. Abbreviations of formation names - Tuscan Nappe: mg = Macigno, cN = Calcareniti a Nummuliti, sp = Scisti Policromi, cma = Maiolica, di = Diaspri, mP = Marne a Posidonia, cst = Calcare Selcifero di Limano, cA Calcari ad Angulati, cm = Calcare Massiccio, cR = Calcari a Rhaetavicula, cc = Calcare Cavernoso (polygenic breccias) (s.l.); Massa Unit: fs = Filladi su-periori, mC = Marmi a Crinoidi e brecce marmoree, fi = Filladi inferiori, b = Paleozoic basement; Apuan Alps Unit: pmg = Pseudomacigno, sc = Scisti Seri¬citici e Cipollini, csE = Calcari Selciferi a Entrochi, d = Diaspri e Scisti Diasprini, cs = Calcari Selciferi e Calcesci¬sti, m = Marmi, md = Marmi Do-lomitici, gr = “Grezzoni”, b = Paleozoic basement.

In this productive aquifer system, the low fracture development at depth enhances a strong non-homogeneity of the groundwater circulation, which is mostly affected by the well-known karst environment (Piccini, 1996; Piccini 1998). As a matter of fact, groundwater mostly flows within well-developed conduit networks, whose arrangement is guided by brittle-regime fractures, and parent faults set. Superficial fracturing, linked to unloading and physical-chemical processes, is responsible for high rates of rainfall infiltration (Doveri et al., 2018b). These features accentuate the "karstic" character of the aquifer system as well reflected in the hydro-physical behaviour of springs. More than 80 springs have flow rates ranging from 10 to 1600 L/s on average and most of them has a high variability index (Tab. 3.1).

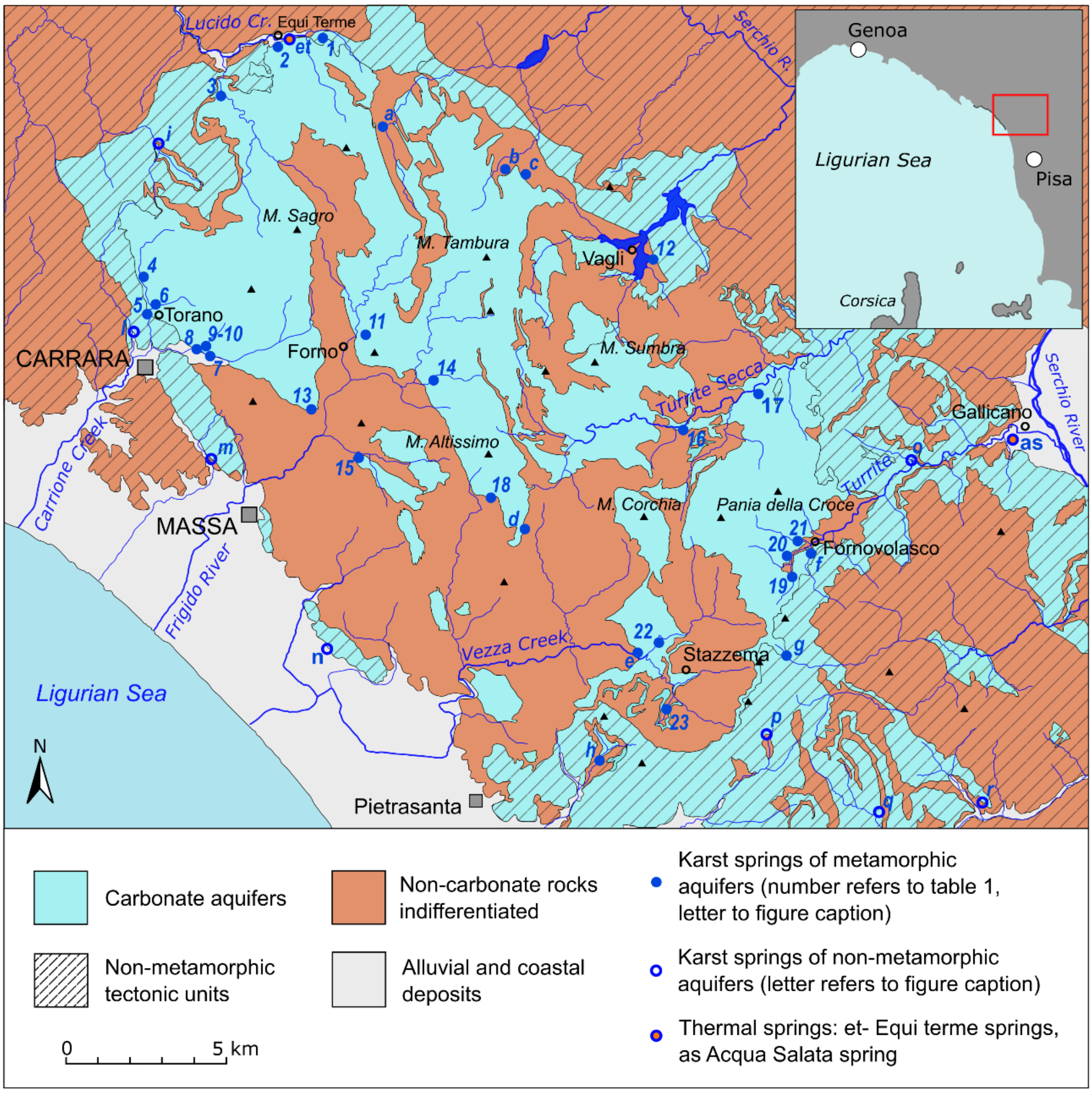

Fig. 3.2 - Hydrogeological sketch map of the Apuan Alps with the position of the major karst springs fed by metamorphic carbonate aquifers (average Q > 10-20 L/s) (from Doveri et al., 2018b). Numbers refer to the codes in Table 3.1. Springs identified by letters are those without hydro-chemical data or fed by non-metamorphic carbonates: ***a*** **-** Tecchiarella (30 L/s), ***b*** **-** Fracassata (30 L/s), ***c*** **-** Preto Marone (20 L/s), ***d*** **-** Polla del Giardino (30 L/s), ***e*** **-** Risvolta (25 L/s), ***f*** **-** Battiferro (40 L/s), ***g*** **-** Botronchio (50 L/s), ***h*** **-** Mulini di S. Anna (50 L/s), ***i*** **-** Tenerano (20 L/S), ***l*** **-** Linara (23 (L/s), ***m*** **-** Materna (20 L/s), ***n*** **-** Porta springs (110 L/s), ***o*** **-** Polla dei Gangheri (300 L/s), ***p*** **-** Grotta all'Onda (70 L/s), ***q*** **-** Campore (30 L/s), ***r*** **-** Trebbio (30 L/s). Thermal springs: **et -** Equi Terme, **as -** Acqua Salata.

Besides than seasonally, the very sensitive behaviour respect to rainfall conditions is also highlighted by the very high variability of flowrate during single rainfall events (Fig. 3.3). These hydrodynamic conditions are moreover well documented by monitoring physical-chemical and isotopic parameters (Doveri et al., 2013c; Piccini et al., 2015; Menichini et al., 2016).

The total discharge of all karst springs amounts to about 5.6 m^3/s, 62% of which is provided by the three major springs: Equi spring (0.8 m^3/s), Polla di Forno (1.6 m^3/s) and Pollaccia (0.9 m^3/s) (Menichini et al., 2016; Piccini, 2002). Most of the karst springs of the Apuan Alps aquifer system is tapped to supply drinking water. Indeed, groundwater hosted in metamorphic carbonate aquifers represents the main source of potable water, used by water-management authorities to supply a wide and densely-populated area in NW Tuscany (nearly 600,000 inhabitants). The main problems of management are linked to high variability of flowrate and the turbidity occurring at springs during storm events, and frequently coupled with bacterial contamination (Drysdale et al., 2001).

Code	Name	Altitude m a.s.l.	Discharge (L/s) n°	avg	Min	Max	$(Q_{max}-Q_{min})/Q_{max}$
1	Palata	450	1	**20**			
2	Equi springs	263	M	**800**	50	16000	0.997
3	Lucido	265	5	**230**	55	500	0.890
4	Carbonera	255	M	**80**	20	150	0.867
5	Tana dei Tufi	165	M	**40**	10	90	0.889
6	Gorgoglio springs group	165	M	**135**	45	350	0.871
7	Martana springs group	200	M	**65**	25	125	0.800
8	Ratto springs	180	M	**180**	100	210	0.524
9	Ravenna	200	5	**10**	5	15	0.667
10	Pero springs	205	5	**22**	10	35	0.714
11	Polla di Forno	230	M	**1600**	135	8000	0.983
12	Aiarone	550	5	**200**	60	350	0.829
13	Cartaro	225	22	**400**	135	800	0.831
14	Renara	283	14	**200**	30	2300	0.987
15	Altagnana	320	9	**60**	13	180	0.928
16	Pollaccia	545	M	**880**	40	6000	0.993
17	Fontanaccio	440	8	**30**	6	400	0.985
18	Polla dell'Altissimo	575	6	**60**	5	100	0.950
19	Chiesaccia	615	6	**150**	65	300	0.783
20	Tana che Urla	600	5	**30**	3	1500	0.998
21	Buca del Tinello	540	6	**20**	2	200	0.990
22	Fontanacce	176	12	**120**	60	500	0.880
23	Mulinette springs	380	5	**80**	15	120	0.875

Tab. 3.1 - Statistical data of discharge for major Apuan springs or group of springs (from Doveri et al., 2018b, modified). Code = spring or springs group number inserted in Fig. 3.2; Vi = variability index (Qmax-Qmin)/Qmax; n° = number of measurements (M indicates continuous monitoring performed at least over one year).

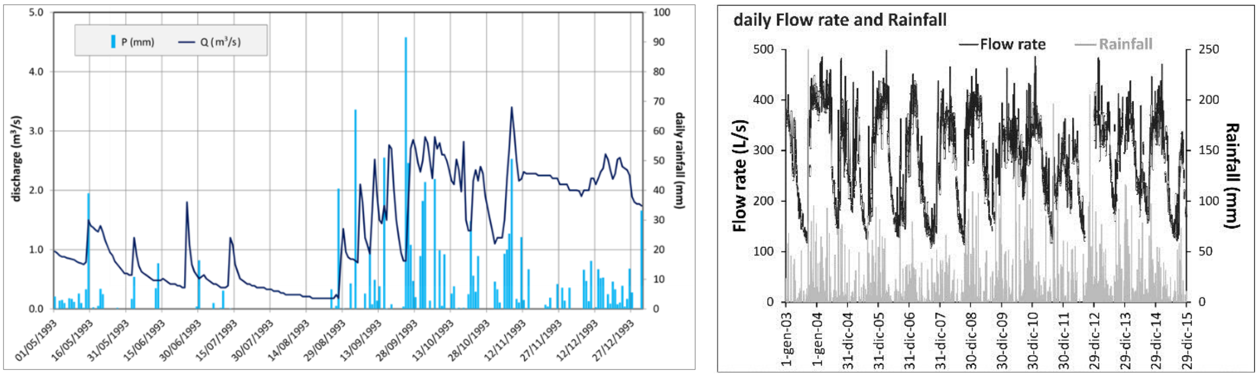

Fig. 3.3 - Rainfall compared to flow rates (Q) of the Pollaccia (left; from Doveri et al., 2018b, modified) and Cartaro (right; from Doveri et al., 2018a) springs. For code and location of the springs, see Tab. 3.1 and Fig. 3.2.

In the last decades, a great number of water-geochemistry surveys were performed over the Apuan Alps area (Orsini, 1987; Doveri, 2000; Doveri, 2004; Mantelli & Piccini, 2007; Menichini, 2012; Mantelli et al., 2015; Molli et al., 2015). Collected data for main springs fed by Apuan Alps aquifer system include 80 chemical analyses of major ions, and 413 analyses on water stable-isotopes ratios (225 and 181, for $\delta^{18}O$‰ and $\delta^{2}H$‰ respectively).

Based on the Piper classification diagram (Fig. 3.4) two main (Ca-HCO_3 and Ca-SO_4), and one intermediate (Ca-HCO_3/SO_4) geochemical facies are evident. Most of studied springs belong to the Ca-HCO3 facies, typical of groundwater that interacts with carbonate rocks. Ca-HCO_3 waters show a range of variation of the Mg/Ca ratio depending on the degree of their interaction with metamorphosed dolostones ("Grezzoni"). The Total Ionic Salinity (TIS) of Ca-HCO_3 springs is low, ranging from 4 to 7 meq/L (Fig. 3.4), and the electrical conductivity (EC) ranges from 200 to 300 µs/cm. The only Ca-SO_4 spring is Aiarone-12, which have also an elevated value of TIS (close to 30 meq/L). According to hydrogeological structures this chemical composition likely results from an interaction of groundwater with the Triassic evaporitic series of the Tuscan Nappe, in the final part of a circuit mainly developed into metamorphic-carbonates (Doveri et al., 2018b).

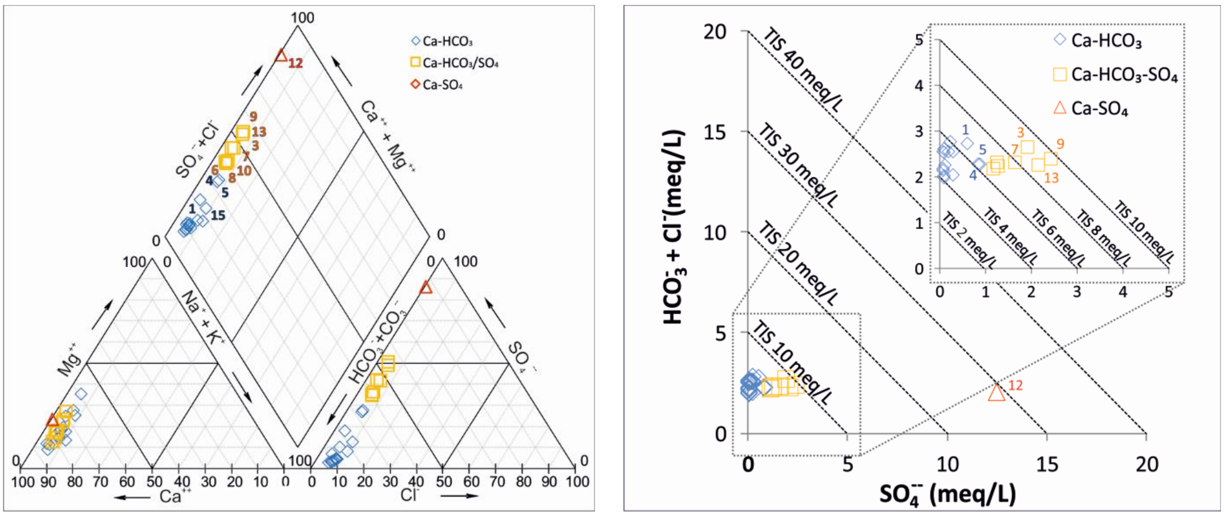

Fig. 3.4 - Chemical classification diagram (left) and "HCO_3 + Cl vs. SO_4" diagram (right; TIS = total ionic salinity) (from Doveri et al., 2018b). For code and location of the springs, see Tab. 3.1 and Fig. 3.2.

The $Ca\text{-}HCO_3/SO_4$ waters have an intermediate value of TIS (7-10 meq/L), and EC higher than $Ca\text{-}HCO_3$ facies (ranging from 300 to 375 µs/cm). This higher value of salinity is chiefly due to higher concentrations of SO_4, as Fig. 3.4 shows. The SO_4 concentration is in the range of 100-120 mg/L (50% of the anion total content) for Ravenna-9 and Cartaro-13, 80-90 mg/L (over 40 % of the anion total content) for Lucido-3 and Martana-7, and 55-60 mg/L (35 % of the anion total content) for Pero-10, Gorgoglio-6 and Ratto-8. Considering that groundwater feeding these springs flows only in the metamorphic carbonate unit (marble, dolomitic marble and "Grezzoni"), the relatively high concentrations of SO_4 are likely due to an interaction with sulphide minerals, as previous works have shown that these rocks can host pyrite (Cortecci et al., 1985; Mancini, 2004).

As a whole, the spring waters cover wide ranges of water stable-isotopes signatures, which range between -6.42 and -7.85‰, and -37.1 and -51.4‰ for $\delta^{18}O$ and $\delta^{2}H$, respectively (Fig. 3.5). These wide ranges are mainly linked to the altitude effect, and to the exposure (seaward or inland) of the hydrogeological basins (Mussi et al, 1998; Menichini, 2012; Doveri et al., 2013c). As generally observed for groundwater in Tuscany (Doveri & Mussi, 2014 and references therein), in the $\delta^{2}H$ vs $\delta^{18}O$ diagram (Fig. 3.5) the points representative of the Apuan springs lie between the Mediterranean Meteoric Water Line (MMWL; Gat & Carm, 1970) and the Global Meteoric Water Line (GMWL; Craig, 1961), thus inferring the origin of rainfall from both the Atlantic Ocean and the Mediterranean Sea. The different catchments of the Apuan Alps are strongly differentiated by extension, mean altitudes and exposition, because of the very rugged topography. These features result in spatial variation of the isotopic fractionation, thus enhancing the usefulness of water isotopes as natural tracers to define groundwater systems.

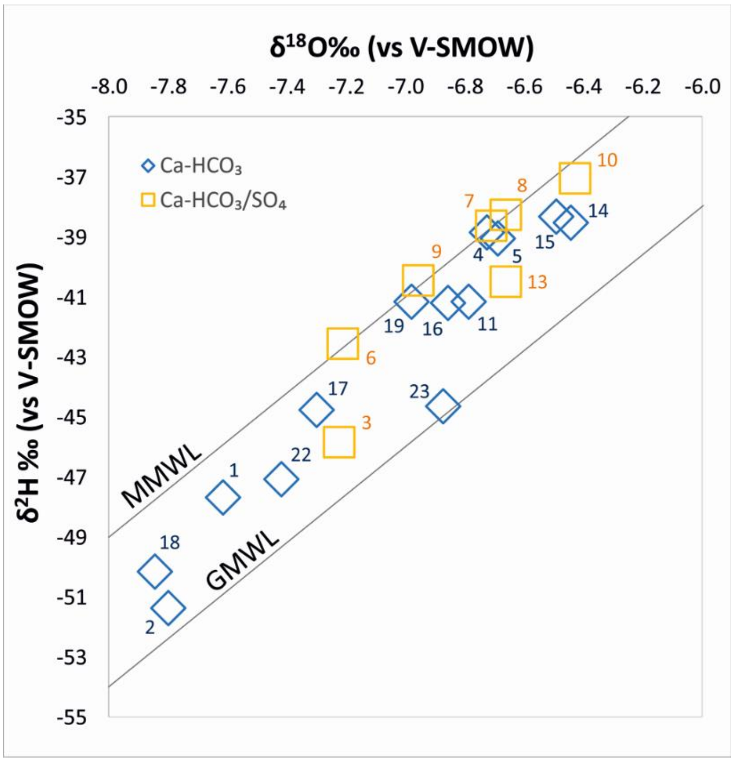

Fig. 3.5 - $\delta^{18}O$‰ vs. $\delta^{2}H$‰ for major springs of the Apuan Alps aquifer system (from Doveri et al., 2018b). For code and location of the springs, see Tab. 3.1 and Fig. 3.2.

3.2. Synthesis of data and information into the aquifer conceptual model

The Apuan Alps contain several explicative cases of metamorphic carbonate aquifers. The high rainfall rate, and the permeable outcropping carbonate rocks (i.e. marble, dolomitic marble and dolomite) result in a figurative “groundwater tower” (5.6 m^3/s as total discharge through the karst springs) that plays a strategic role for supplying water to the surrounding inhabited areas. In these rocks the surficial fracturing is responsible for high rates of diffuse infiltration, whereas the low development of fractures at depth, and the low porosity of the matrix, promote a groundwater flow within low-density networks of well-developed karst conduits. Hence, with the exception of local situations, the hydrodynamic behaviour of the Apuan metamorphic aquifers is characterized by enhanced karstic behaviour, as shown by springs which have a high variability of both flow rates and geochemical characteristics. Despite incomplete records, the monitoring of springs clearly suggests that the metamorphic carbonate aquifers of the Apuan Alps have a weak storage capacity for supplying the base flow, thus leading to early breakthrough of low flow at springs following the wet season (November-April). Base flows of the aquifers are likely to be more related to the release of water stored in the epikarst, rather than to the emptying of minor fractures in the saturated zone. The general variability of water isotopes signatures observed over time at springs is in agreement with this conceptual model, considering it requires relatively short transit times of the groundwater flow drained by the springs. Another aspect, which is consistent with the absence of pervasive fracturing in the saturated zone, and with a well-organized groundwater flow occurring along main karst fractures and conduits, is the significant difference of isotope signatures of springs very close to each other. Overall, these features make the aquifers highly vulnerable to contamination, and particularly sensitive to climate changes. Since the Apuan Alps also contain valuable stones for ornamental purposes (e.g. the Carrara Marble), and the activities for quarrying this economic resource is widely diffused, such vulnerability translates into a risk, as evidenced by the frequent occurrences of high-turbidity at springs, and by the sporadic contamination from hydrocarbon in these waters. These phenomena exacerbate the already difficult conditions of managing karst groundwater sources, and underscore the importance of gathering additional knowledge on these complex aquifer systems, in order to improve the planning of quarrying activities. As suggested by the results presented in this chapter, a comprehensive approach that involves geological, hydro-physical and geochemical tools are strongly recommended for managing water supplies in the complex metamorphic carbonate aquifers.

3.3. Data of monitoring and trends

As regards the trend over time of groundwater quantity and chemical compounds concentration, for this aquifer system a preliminary elaboration (by the same methodology discussed in § 2.3) has been performed for the Cartaro spring (n. 13 in Fig. 3.2 e Tab. 3.1), the most important spring among those tapped for drinking water in the Apuan Alps area. Monitoring data of spring discharge are available tanks to the water management society (GAIA SpA), rainfall and air temperature data are from the Hydric Service of the Tuscany

Region authority (SIR) and the chemical data of the spring water from the environmental agency of Tuscany (ARPAT).

As regards the water chemistry, at present only the evolution of Cl concentration has been accounted, without a statistically consistent trend (Test Theil-Sen), even though a slight tendency of decreasing seems to exist (Fig. 3.6).

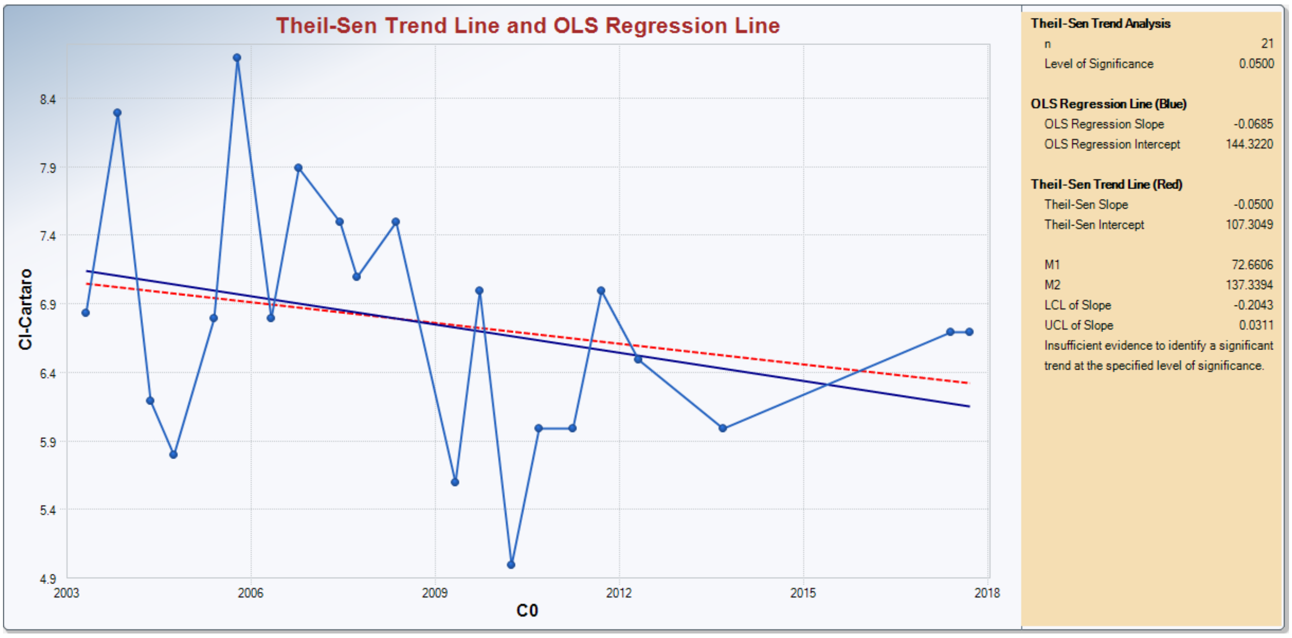

Fig. 3.6 - Time series of the Cl concentration in the Cartaro spring. The dashed red line refers to Theil-Sen test, while the blue line refers to OLS Regression.

Similarly, the statistical test doesn't show a significant trend neither for the spring discharge or rainfall. A preliminary evaluation of the monthly effective rainfall was done by the Thornthwaite & Mather (1955). In agreement with the hydrodynamic conditions typical of karst aquifers, a robustness, and practically in phase, relationship is observed between the spring flow rate and effective rainfall (Fig. 3.8). Even if over seasons a variability of the effective rainfall occurs, in first instance a "4 months- moving average" calculated on this parameter seems to describe enough well the evolution of the spring discharge, thus pointing out the very different behaviour of this system respect to that of the Mt. Amiata aquifer.

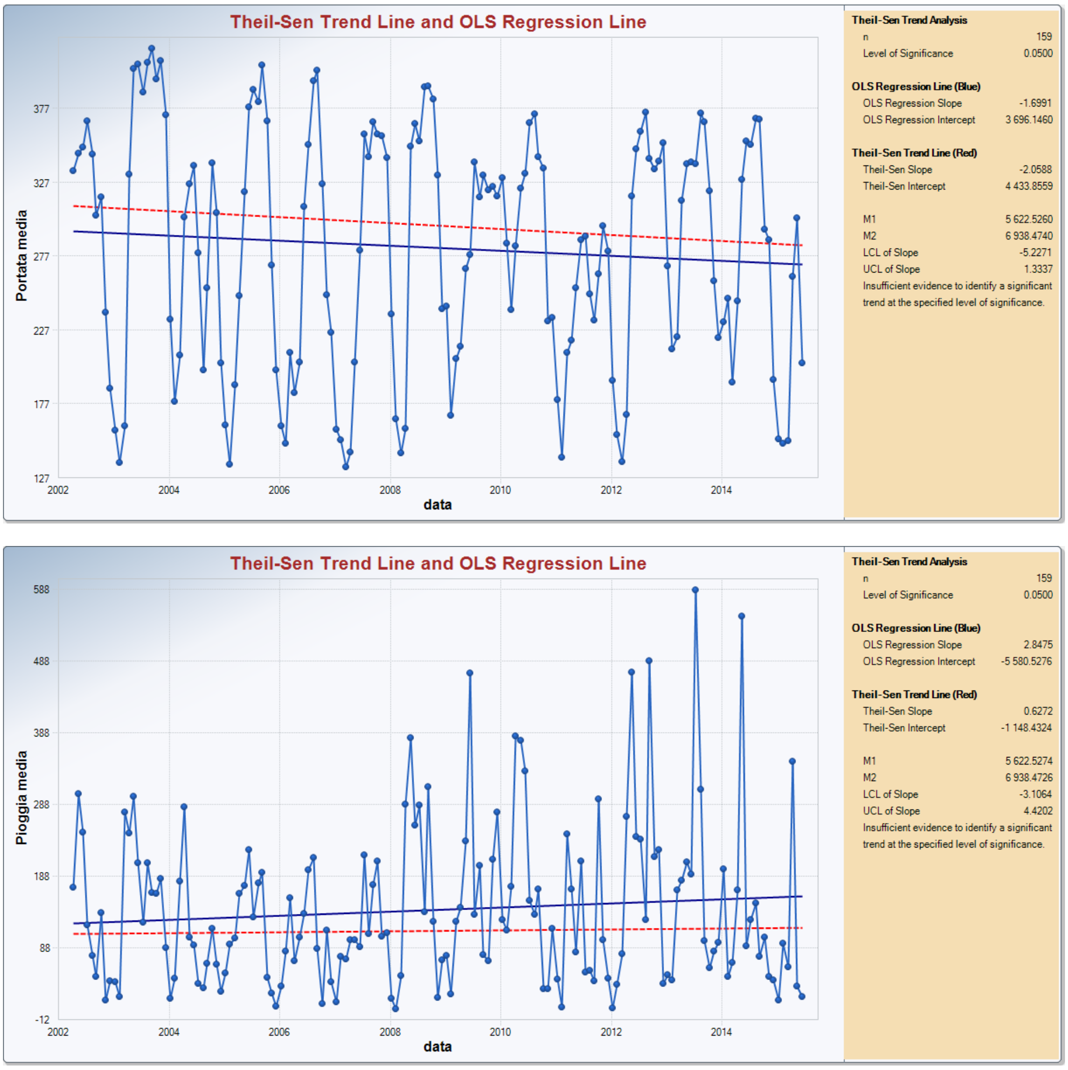

Fig. 3.7 – Time series of monthly rainfall (lower diagram) and Cartaro-spring flow rate (upper diagram) over the 2002-2015 period. The dashed red line refers to Theil-Sen test, while the blue line refers to OLS Regression.

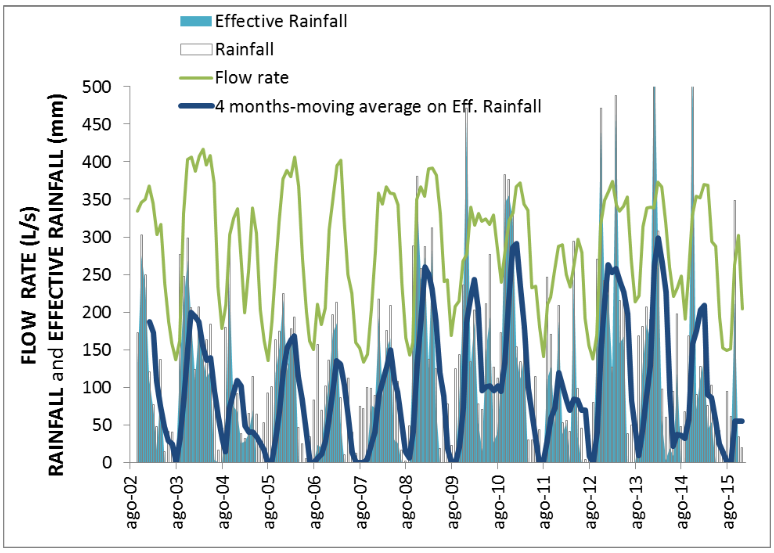

Fig. 3.8 – Time series of monthly rainfall, effective rainfall and Cartaro-flow rate over the 2002-2015 period. A curve of 4 months-moving average on effective rainfall values is also showed.

4. CONCLUSION

The aquifer systems accounted in the project have been examined from different points of view, considering geological, hydrogeological and hydraulic-hydrodynamic features, as well as chemistry and water isotopes signature of groundwater.

This comprehensive approach steered the definition of the aquifer conceptual model, comprising the kind of rocks hosting groundwater and their hydraulic properties, the arrangement of groundwater flow, the seasonal evolution of groundwater quantity and the chemical quality of groundwater.

The statistical analysis performed on datasets from monitoring stations highlighted some trends over decades. One of the most significant is the decreasing of groundwater yield registered in central Apennines for the volcanic aquifer of Mt. Amiata over the 1990-2010 period, which has been followed by a recovery of flow rates in the successive six-seven years. A qualitative relationship between this behaviour with the evolution of effective rainfall has been preliminary individuated, underlining as the discharge at major springs is mainly affected by an infiltration occurred over a period of about two years.

From a water quality point of view, local geochemical background threshold limits were defined for more significant compounds and parameters. Some trends of the physical-chemical and chemical features were also individuated. One of the most significant is the Cl concentration increasing observed at some monitored springs.

Next steps of the work will consist in refinements of the relationships among meteo-climatic parameters and quantity and quality groundwater parameters, and in the development of numerical models able to reproduce the groundwater yield evolution as well.

5. REFERENCES

Acocella, V. (2000): Space accommodation by roof lifting during pluton emplacement at Amiata (Italy). Terra Nova, 12, 149–155.

Apollaro C., Accornero M., Marini L., Barca D., De Rosa R. (2009) The impact of dolomite and plagioclase weathering on the chemistry of shallow groundwaters circulating in a granodiorite-dominated catchment of the Sila Massif (Calabria, Southern Italy). Appl. Geochem., 24, 957-979.

Appelo C.A.J. and Postma D. (1996) Geochemistry, groundwater and pollution. A.A. Balkema, Rotterdam.

Baldi, P., Bellani, S., Ceccarelli, A., Fiordelisi, A., Squarci, P. & Taffi, L. (1995): Geothermal anomalies and structural features of southern Tuscany. World Geothermal Congress Proceedings Florence, pp 1287–1291.

Balestro G., Cadoppi P., Piccardo G.B., Polino R., Spagnolo G., Tallone S., Fioraso G., Lucchesi S., Forno M.G. (2009) Geological map of Italy at the scale 1:50:000, sheet 155 Torino Ovest. ISPRA, Istituto Superiore per la Protezione e la Ricerca ambientale, Roma.

Baoxiang Z., Fanhai M. 2011. Delineation methods and application of groundwater source protection zone. Water Resource and Environmental Protection (ISWREP), 2011 International Symposium on Volume: 1 (IEEE Conference Publications): pp 66–69

Barazzuoli P., Bosco G., Nante N., Rappuoli D. e Salleolini M. (1994) The aquifer of Mount Amiata: Evaluation of the perennial yield and its quality. Mem. Soc. Geol. It., 48, 825-832.

Barazzuoli P., Capacci F., Gobbini M., Migliorini J., Rigati R. e Mocenni B. (2014) Valutazioni delle risorse idriche dell'acquifero contenuto nelle vulcaniti del Monte Amiata attraverso criteri strettamente idrologici. Il Geologo, Anno XXV, 94, 5-13.

Batini, F., Bertini, G., Gianelli, G., Nicolich, R., Pandeli, E. & Puxeddu, M. (1986): Deep structure of the geothermal region of the Monte Amiata volcano (Tuscany, Italy). Mem. Soc. Geol. It., 35, 755–759.

Boccaletti, M., Elter, P. & Guazzone, G. (1971): Plate Tectonics models for the development of the western Alps and Northern Apennines. Nature, 234, 108-111.

Bolviken B., 1971. A statistical approach to the problem of interpretation in geochemical prospecting. Can. Inst. Min. Met., Spec. Vol. 11, 564-567.

Bove A., Casaccio D., Destefanis E., De Luca D.A., Lasagna M., Masciocco L., Ossella L., Tonussi M. (2005) Idrogeologia della pianura piemontese. Regione Piemonte Direzione Pianificazione delle Risorse Idriche, Mariogros Industrie Grafiche S.p.A., Torino.

Brogi, A. (2008): The structure of the Monte Amiata volcano-geothermal area (Northern Apennines, Italy): Neogene- Quaternary compression versus extension. Int. J. Earth Sci., 97, 677–703.

Brunet, C., Monie´ , P., Jolivet, L. & Cadet, J.P. (2000): Migration of compression and extension in the Tyrrhenian Sea: insights from 40Ar / 39Ar ages on micas along a transect from Corsica to Tuscany. Tectonophysics, 321, 127–155.

Canavese P.A., De Luca D.A., Masciocco L. (2004) La rete di monitoraggio delle acque sotterranee delle aree di pianura della Regione Piemonte: quadro idrogeologico. Prismas: il monitoraggio delle acque sotterranee nella Regione Piemonte, Regione Piemonte, 175pp.

Capilongo L., Cotterchio C., Faliero P., Ferrero C., Latagliata V., Pantaleo B., Rinaldi A., Bortolami G., De Luca D.A., Masciocco L., Morelli A. (2003) Le acque sotterranee della pianura di Torino - Carta della base dell'acquifero superficiale - Note illustrative.

Carmignani L., Kligfield R. 1990. Crustal extension in the Northern Apennines: the transition from compression to ex-tension in the Alpi Apuane Core Complex. Tectonics, v. 9, 6, 1275-1303.

Carmignani, L., Decandia, F.A., Disperati, L., Fantozzi, P.L., Lazzarotto, A., Liotta, D. and Oggiano, G. (1995): Relationships between the Sardinia-Corsica-Provencal Domain and the Northern Apennines. Terra Nova, 7, 128–137.

Celico P.B. (1987) Piano di Bacino del Fiume Fiora: studio idrogeologico preliminare. Relazione tecnica, VAMS Ingegneria s.r.l. - Ministero dei Lavori Pubblici Provveditorato alle OO.PP per la Toscana, pp. 50.

Cerrina F. A., Da Prato S., Doveri M., Ellero A., Lelli M., Marini L., Masetti G., Nisi B. e Raco B. (2009). Caratterizzazione geologica, idrogeologica e idrogeochimica dei Corpi Idrici Sotterranei Significativi della Regione Toscana (CISS) 99MM020 "Acquifero dell'Amiata". Report Regione Toscana, p. 44.

Chiodini G., Frondini F., Marini L. (1995) Theoretical geothermometers and PCO2 indicators for aqueous solutions coming from hydrothermal systems of medium-low temperature hosted into carbonate-evaporite rocks. Application to the thermal springs of the Etruscan Swell, Italy. Appl. Geochem., 10, 337-346.

Civita M., Forti P., Marini P., Meccheri M., Micheli L., Piccini L., Pranzini G. 1991. Carta della vulnerabilità all'inquinamento degli acquiferi delle Alpi Apuane "Pollution Vulnerability map for the aquifers of the Apuane Alps" – scala "scale" 1:25.000. Gruppo Nazionale per la Difesa dalle Catastrofi Idrogeologiche, C. N. R., SE.L.CA, Firenze.

Conti P., Di Pisa A., Gattiglio M., Meccheri M. 1993. Prealpine basement in the Alpi Apuane (Northern Apennines, Italy). In: Von Raumer, J.F., Neubauer, F. (Eds.), Pre-Mesozoic geology in the Alps. Springer Verlag, 609-621.

Cortecci G., Lattanzi P., Tanelli G. 1985. Barite-iron oxide-pyrite deposits from Apuane Alps (Northern Tuscany, Italy). Geol. Carpatica, 36, 347-357.

Craig H. 1961. Isotopic Variation in meteoric waters. Science, 133, 1702-1703.

De Luca D. A., Osella L. (2014) Assetto idrogeologico della Città di Torino e del suo hinterland. Geologia dell'Ambiente, Atti del simposio "Geologia urbana di Torino", 1/2014: 10-15.

De Luca, D. A., Destefanis, E., Forno M. G., Lasagna, M., Masciocco, L., (2014) The genesis and the hydrogeological features of the Turin Po Plain fontanili, typical lowland springs in Northern Italy. Bull Eng Geol Environ 73:409–427.Lo Russo S., Taddia G. (2009) Groundwater in the Urban Environment:Management Needs and Planning Strategies. Am. J. Environ. Sci., 5(4): 484-500

Doveri M. 2004. Studio idrogeologico e idrogeochimico dei sistemi acquiferi del bacino del Torrente Carrione e dell'antistante piana costiera. Tesi di Dottorato inedita, Università di Pisa, 178 pp.

Doveri M. e Mussi M. (2014) Water Isotopes as Environmental Tracers for Conceptual Understanding of Groundwater Flow: An Application for Fractured Aquifer Systems in the "Scansano-Magliano in Toscana" Area (Southern Tuscany, Italy). Water, 6, 2255-2277.

Doveri M., 2000. Studio idrogeochimico di sistemi acquiferi superficiali e profondi delle Alpi Apuane e della Valle del Serchio. Tesi di Laurea, Università di Pisa, a.a. 1999-2000, 245 pp.

Doveri M., Grassi S., Menichini M. e Bellatalla M. (2013a) Dati e considerazioni a carattere idrodinamico sulle vulcaniti del Monte Amiata (Toscana meridionale). Convegno IdroVulc2013, Riassunti, 71-73.

Doveri M., Menichini M. (2017) Aspetti idrogeologici delle vulcaniti nel Monte Amiata. In: Il Vulcano di Monte Amiata. a cura di Claudia Principe, Guido Lavorini e Luigina M. Vezzoli (eds.), pp. 255 - 265. ESA - Edizioni Scientifiche ed Artistiche, 2017 - Napoli, Italia.

Doveri M., Menichini M., Cerrina Feroni A. 2013c. Stable water isotope as foundamental tool in karst aquifer studies: some results from isotopic applications in the Apuan Alps carbonatic complexes (NW Tuscany). Italian Journal Engineering Geology and Environment 1: 25-42.

Doveri M., Menichini M., Provenzale A., Scozzari A. (2017) Effects of climate change on groundwater: observed and forecasted trends on Italian systems. EGU General Assembly Conference Abstracts, 19, 14440

Doveri M., Menichini M., Provenzale A., Scozzari A. (2018a) Groundwater response to climate changes: examples of observed and modeled trends on Tuscany aquifers (central Italy). Volume Atti Accademia Lincei giornata mondiale sull'acqua 2017, in press.

Doveri M., Menichini M., Scozzari A. 2016. Protection of groundwater resources: worldwide regulations, scientific approaches and case study. In: Scozzari A, Dotsika E (edited by): "Threats to the quality of groundwater resources: prevention and control" - The handbook of environmental chemistry, Springer-Verlag Berlin Heidelberg 2016, 40,13-30.

Doveri M., Nisi B., Cerrina Feroni A., Ellero A., Menichini M., Lelli M., Masetti G., Da Prato S., Principe C., Raco B. (2012). Geological, hydrodynamic and geochemical features of the volcanic aquifer of Mt. Amiata (Tuscany, Central Italy): an overview. Acta Vulcanologica, Vol.24 (1-2), pp. 51-72.

Doveri M., Nisi B., Ellero A., Menichini M., Lelli M., Masetti G., Da Prato S. e Raco B. (2013b) Geological-hydrogeological-geochemical integrated approach to characterize Significant

Groundwater Bodies hosted in fractured rocks: the example of the Monte Amiata volcanic aquifer (Tuscany, Italy). Epitome Geoitalia 2013, 269.

Doveri, M., Piccini, L., Menichini, M. (2018b) Hydrodynamic and geochemical features of metamorphic carbonate aquifers and implications for water management: the Apuan Alps (NW Tuscany-Italy) case study. In: Karst Water Environment: Advances in Research, Management and Policy (T. Younos, M. Schreiber, K. K. Ficco, Editors). Springer Publishers (in press).

Drysdale R. N., Pierotti L., Piccini L., Baldacci F. 2001. Suspended sediments in karst spring waters near Massa (Tuscany), Italy. Environmental Geology 40, 1037-1050.

Fan Y. 2015. Groundwater. How much and how old? News & Views, Nature Geoscience, advance online publication, www.nature.com/naturegeoscience, 1-2.

Ferrari, L., Conticelli, S., Burlamacchi, L. & Manetti, P. (1996): Volcanologic evolution of the Monte Amiata, Southern Tuscany: new geological and petrochemical data. Acta Vulcanol., 8, 41–56.

Frondini F., Caliro S., Cardellini C., Chiodini G., Morgantini N. (2009) Carbon dioxide degassing and thermal energy release in the Monte Amiata volcanic-geothermal area (Italy). Appl. Geochem., 24, 860-875.

Gambardella B., Marini L. Baneschi I., (2005) Dissolved potassium in the shallow groundwaters circulating in the volcanic rocks of central-southern Italy. Appl. Geochem., 20, 875-897.

Garrels R. M. (1968) Genesis of some ground waters from igneous rocks In Researches in Geochemistry (ed. P. H. Abelson), Vol. 2, pp. 406–420. Wiley.

Gat J.R., Carmi I. 1970. Evolution of isotopic composition of atmospheric waters in the Mediterranean sea area. J. Geophys. Res., 75, 3032-3048.

Gatt J.; Klein B.; Kushnir Y.; Roether W.; Wernli H.; Yam R.; Shemesh A. (2003). Isotope composition of air moisture over the Mediterranean Sea: an index of the air-sea interaction pattern. Tellus B, 55, 953 - 965.

Hiscock K.M. 2011. Groundwater in the 21st century – meeting the challenges. In: Anthony J, Jones A (eds) Sustaining groundwater resources: a critical element in the global water crisis, in International Year of Planet Earth, pp 207–225.

Irace, A. Clemente, P., Piana, F., De Luca, D.A., Polino, R., Violanti, D., Mosca, P., Trenkwalder, S., Natalicchio, M., Ossella, L., Governa, M. & Petricig, M. (2010). Hydrostratigraphy of the late Messinian-Quaternary basins in the southern Piedmont (northwestern Italy). Mem. descr. Carta Geol. It., 90, 133-152, ISSN: 0536-0242.

Irace, A., Clemente, P., Natalicchio, M., Ossella, L., Trenkwalder, S., De Luca, D. A., Mosca, P., Piana, F., Polino, R. & Violanti, D. (2009). Geologia e idrostratigrafia profonda della Pianura Padana occidentale. Edizioni La Nuova Lito, Firenze, 1-135.

Jolivet, L., Daniel, J.M., Truffert, C. & Goffe´ , B. (1994). Exhumation of deep crustal metamorphic rocks and crustal extension in back-arc regions. Lithos, 33, 3–30.

Lelli, M. 2017. Caratterizzazione chimica delle acque circolanti all'interno del Complesso Vulcanico del Monte Amiata. In "Il vulcano di Monte Amiata", Eds. C. Principe, G. Lavorini, L. Vezzoli, pp. 267-280.

Lepeltier C., 1969. A simplified statistical treatment of geochemical data by graphical representation. Econ. Geol., 64, 538-550.

Lucchesi (2001) Sintesi preliminare dei dati di sottosuolo della pianura piemontese centrale. Ge.am, 103, 115-121

Mancini S., 2004. La buca dell'Angina grotta e miniera apuana. www.alpiapuane.info.

Mantelli F., Lotti L., Montigiani A., Piccini L. 2015. Chimica delle acque del Complesso carsico del Monte Corchia. Acta Apuana, XI (2012), 33-45.

Mantelli F., Piccini L. 2007. Caratteristiche chimiche delle acque delle sorgenti carsiche delle Alpi Apuane. In: Comitato Alpi Apuane 2007, "Apuane e dintorni – Guida incompleta al fenomeno carsico", Tip. Amaducci, Borgo a Mozzano, Lucca, 69-75.

Marroni M., Moratti G., Costantini A., Conticelli S., Benvenuti M. G., Pandolfi L., Bonini M., Cornamusini G. e Laurenzi M. A. (2015) Geology of the Monte Amiata region, Southern Tuscany, Central Italy. Ital. J. Geosci., 134, 171-199.

Martinetto E., Scardia G., Varrone D. (2007) Magnetobiostratigraphy of the Stura di Lanzo fossil forest succession. Riv. Ital. Paleontol. Stratigr. 113 (1), 109–125.

Martınez Navarrete C., Grima Olmedo J, Duran Valsero J.J., Gomez J.D., Luque Espinar J.A., de la Orden G.J.A. 2008. Groundwater protection in Mediterranean countries after the European water framework directive. Environ Geol 54:537–549.

Menichini M. 2012. A multidisciplinary approach to defi ne the hydrogeological model of aquifer systems in the "Fiume Versilia" catchment and the adjacent coastal plain (Northwest Tuscany, Italy). Tesi di Dottorato inedita, Università di Pisa, Scuola di Dottorato Galileo Galilei. Programma in Scienze della Terra.

Menichini M., Doveri M., Piccini L. 2016. Hydrogeological and geochemical overview of the karst aquifers in the Apuan Alps (Northwestern Tuscany, Italy). Italian Journal of Groundwater, AS16-198: 15-23.

Minissale A., Magro G., Vaselli O., Verrucchi C., Perticone I. (1997). Geochemistry of water and gas discharges from the Mt. Amiata silicic complex and surrounding areas (central Italy). Journal of Volcanology and Geothermal Research, 79, 223 -251.

Molli G., Cortecci G., Vaselli L., Ottria G., Cortopassi A., Dinelli E., Mussi M., Barbieri M. 2010. Fault zone structure and fluid-rock interaction of a high angle normal fault in Carrara marble (NW Tuscany, Italy). Journal of Structural Geology 32, 1334-1348.

Molli G., Doveri M., Manzella A., Bonini L., Botti F., Menichini M., Montanari D., Trumpy E., Ungari A., Vaselli L. 2015. Surface - subsurface structural architecture and groundwater flow of the Equi Terme hydrothermal area, northern Tuscany Italy, Italian Journal of Geosciences, vol. 134, 442-457.

Molli G., Meccheri M. 2012. Structural inheritance and style of reactivation at mid-crustal levels: A case study from the Alpi Apuane (Tuscany, Italy). Tectonophysics 579, 74-87.

Molli, G. (2008): Northern Apennine–Corsica orogenic system: an updated review. Geol. Soc. London Spec. Publ., 298, 413– 442.

Mussi M., Leone G., Nardi I. 1998. Isotopic geochemistry of natural water from the Alpi Apuane- Garfagnana area, Northern Tuscany, Italy. Miner. Petrogr. Acta 41, 163-178.

Orsini A. 1987. Indagine idrogeologica e geochimica ai fini della ricostruzione dei bacini di alimentazione di alcuni sorgenti nella zona delle Apuane. Tesi di laurea in Scienze Geologiche, Facoltà di Scienze M.F.N., Università degli Studi di Firenze, 124 pp.

Ottria, G., Molli G. 2000. Superimposed brittle structures in the late-orogenic extension of the Northern Apennine: results from the Carrara area (Alpi Apuane, NW Tuscany). Terra Nova 12: 52-59.

Piana, F., Fioraso, G., Irace, A., Mosca, P., d'Atri, A., Barale, L., Falletti, P., Monegato, G., Morelli, M., Tallone, S., Vigna, G.B., 2017. Geology of Piemonte region (NW Italy, Alps-Apennines interference zone). J. Maps 13 (2), 395–405.

Piccini L. 2002. Acquiferi carbonatici e sorgenti carsiche delle Alpi Apuane "Carbonate aquifers and karst springs of Apuan Alps". Atti Conv. "Le risorse idriche sotterranee delle Alpi Apuane: conoscenze attuali e prospettive di utilizzo", Forno di Massa, Giugno 2002: 41-76.

Piccini L., Giannini E., Malcapi V., Poggetti E., Steinberg B. 2015. Monitoraggio idrodinamico di un sistema carsico: risultati preliminari di un anno d'indagini alla sorgente Pollaccia (Alpi Apuane – Toscana). Atti Convegno "La ricerca carsologica in Italia", Fabrosa Soprana (CN), 22-23 giugno 2013, 147-154.

Piccini L., Pranzini G., Tedici L., Forti P. 1999. Le risorse idriche dei complessi carbonatici del comprensorio apuo-versiliese "water resources of carbonate complexes in apuan-versilian region". Quaderni Geologia Applicata 6-1, 61-78.

Principe C., Vezzoli L., La Felice S. (2017) Stratigrafia ed evoluzione geologica del vulcano di Monte Amiata. In: Il Vulcano di Monte Amiata. a cura di Claudia Principe, Guido Lavorini e Luigina M. Vezzoli (eds.), pp. 85 - 101. ESA - Edizioni Scientifiche ed Artistiche, 2017 - Napoli, Italia.

Rosegrant M.W., Cai X., Cline S.A. 2002. World Water and Food to 2025: dealing with scarcity. International Food Policy Research Institute, Washington, 322 pp.

Siebert S, Burke J, Faures J M, Frenken K, Hoogeveen J, Döll P, Portmann F T (2010) Groundwater use for irrigation – a global inventory. Hydrol Earth Syst Sci, 14: 1863-1880.

Sinclair A.J., 1974. Selection of thresholds values in geochemical data using probability graphs. Journal of Geochemical Exploration, 3, 129-149.

Sinclair A.J., 1976. Application of probability graphs in mineral exploration. Special Volume No. 4. The Association of Exploration Geochemists. Canada. 95 pp.

Sinclair A.J., 1986. Statistical interpretation of soil geochemical data, 97-115. In: Exploration geochemistry: design and interpretation of soil surveys. (W.K. Fletcher, S.J. Hoffman, M.B.

Tassi F., O. Vaselli, F. Cuccoli, A. Buccianti, B. Nisi, E. Lognoli and G. Montegrossi. 2009. A geochemical multi-methodological approach in hazard assessment of CO2-rich gas emissions at Mt. Amiata volcano (Tuscany, central Italy). Water Air Soil Poll. Focus, 9, 117-127. DOI10.1007/s11267-008-9198-2.

Taylor R., Scanlon B., Doll P., Rodell M. et al. 2013. Ground water and climate change. Nature climate change, 3:322-329

Tennant C.B., White M.L., 1959. Study of the distribution of some geochemical data. Econ. Geol., 54, 1281-1290.

Vaselli L., Cortecci G., Tonarini S., Ottria G., Mussi, M. 2012. Conditions for veining and origin of mineralizing fluids in the Alpi Apuane (NW Tuscany, Italy): Evidence from structural and geochemical analyses on calcite veins hosted in Carrara marbles. Journal of Structural Geology 44, 76-92.

Vaselli, O., Rappuoli, D., Nisi, B., Bianchi, F., Tassi, F., Cabassi, J., Giannini, L., Magi, F., Capecchiacci, F., Maddii, V., 2017. Geochimica delle acque di Galleria Italia (Abbadia San Salvatore, Siena). In "Il vulcano di Monte Amiata", Eds. C. Principe, G. Lavorini, L. Vezzoli, pp. 283-302.

VV. AA. 2010. "Indagine geochimica ed isotopica delle acque termo- ed oligo-minerali dell'area amiatina. MAC-GEO Project, Regione Toscana, 45 pp.

WBCSD, 2006. Facts and trends – water. World Business Council for Sustainable Development. http://www.wbcsd.org/Pages/EDocument/EDocumentDetails.aspx?ID=137. Accessed 10 Sept 2014.

Wolery T.W., Jarek R.L., 2003. Software user's manual. EQ3/6, Version 8.0. Sandia National Laboratories – U.S. Dept. of Energy Report.

Zhu Y. Balke K. D. 2008. Groundwater protection: what can we learn from Germany? J. Zhejiang Univ Sci B 9(3):227–231.